

Paleointensity Determination and Rock-magnetic Characters of Piton de la Fournaise 1998 Lava, Reunion Island

Naoko UENO*, Zhong ZHENG**

Abstract

Geomagnetic intensity of Piton de la Fournaise 1998 lava in Reunion Island was investigated by using the Zheng's method for paleointensity study. An excellent result of $36.1 \pm 1.9 \mu\text{T}$ was obtained. For reference, a differentiated Thelliers' method yielded $37.7 \pm 4.2 \mu\text{T}$, and the total intensity of the IGRF 2000 model field at the sampling point is calculated to $36.4 \mu\text{T}$

Key words: Reunion1998 lava, Paleointensity, Differentiated Thellier method, Zheng method

1. Introduction

The new method developed by Zheng (Zheng et al., 2005; Ueno et al., 2008; Ueno and Zheng, 2010) was applied for paleointensity determination on the basaltic rocks erupted in 1998, at Piton de la Fournaise in Reunion Island, Indian Ocean.

Samples were collected during the 1998 eruption at (h=2630m height, 21.14S, 55.43E), where the total intensity of the IGRF 2000 model is calculated to $36.4 \mu\text{T}$.

Results by the differentiated Thelliers' method were illustrated for comparison.

2. Samples and rock magnetic characters

Samples were collected during the eruption of Piton de la Fournaise in 1998, while the field excursion promoted by the International Volcanological Congress (IAVCEI '98, Cape Town) was going on. The title of the excursion was the "A6: Volcanic Geology of Reunion Island, Indian Ocean". Sampling site is shown in Fig. 1 (Fig.1-1, Fig.1-2, Fig.1-3). All of the

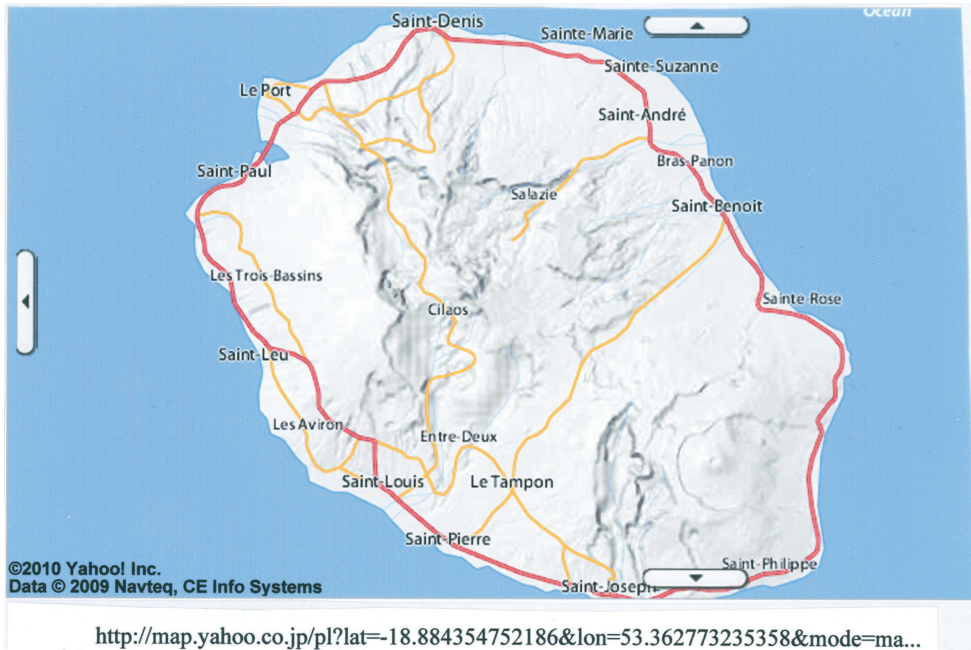
*) 上野直子：東洋大学自然科学研究室 〒112-8606 東京都文京区白山 5-28-20
Natural Science Laboratory, Toyo University, 5-28-20, Hakusan, Bunkyo-ku, Tokyo, 112-8606 JAPAN
E-mail: ueno@toyo.jp

**) 鄭重：綜合開発株式会社地球科学事業部 〒133-0057 東京都江戸川区西小岩 1-30-16 三幸ビル 2 号館
Sogo Kaihatu Co., Sanko Buil., 1-30-16, Nishikoiwa, Edogawaku, Tokyo, 133-0057 JAPAN
E-mail: tei-cho@sogo-geo.co.jp

Fig. 1 Sampling site



<http://map.yahoo.co.jp/print?lat=-18.88435540818169&lon=53.362772828294&z=7...>



<http://map.yahoo.co.jp/pl?lat=-18.884354752186&lon=53.362773235358&mode=ma...>

Fig. 1-1 Location of Reunion Island (copied from map.yahoo)

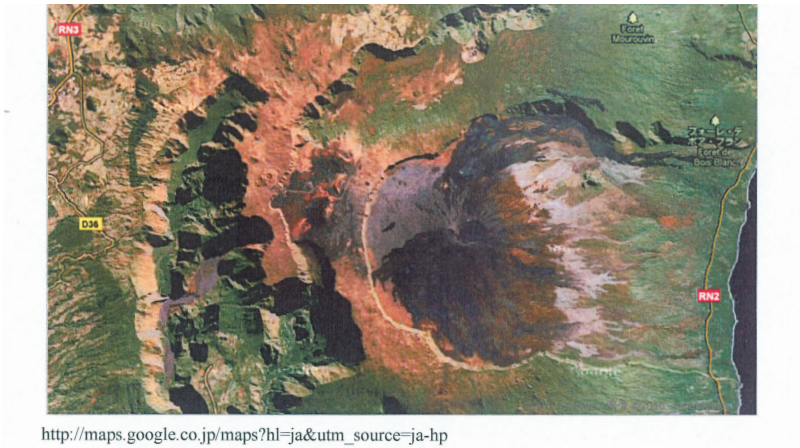


Fig. 1-2 Map of Piton de la Fournaise in Reunion Island (copied from maps. google)

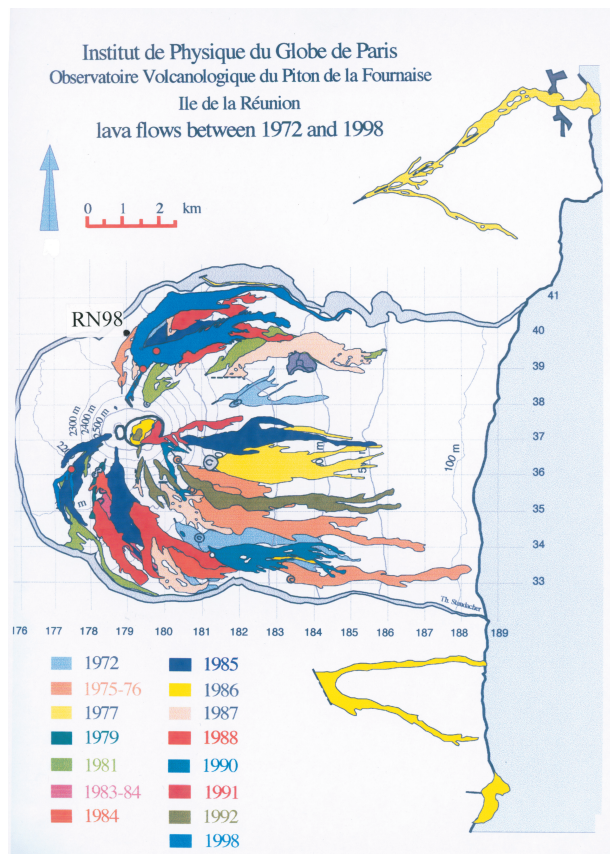


Fig. 1-3 Sampling site (original map: Thomas Staudacher, 1998)



Fig. 2-1 Photograph of RN98_H3

samples were still warm which erupted in a few days before sampling. Samples were numbered RN98_H1 ~ H3. The high density specimens numbered from RN98_H3-1 to H3-6 were mainly used for analysis (Fig.2-1).

Microscopic observations:

Fig.2-2 shows microscopic observation of some specimens under plane-polarized light and crossed polar. Fig.2-3 is the back scatter image (BEI) by scanning electron microscope of RN98_H3-1 ~ H3-6. From these figures, delicate skeletal titanomagnetite crystals are considered to be the main carrier of remanent magnetization.

Thermal Demagnetization:

Zijderveld diagram (Zijderveld, 1967) and unblocking temperature spectra of NRM on the high density block (Fig.3-1) and the porous block named RN-P (Fig.3-2) are shown. These figures provide the preliminary information of thermal remanent characters to arrange the proper temperature steps. Both of the two blocks have the two unblocking temperature spectra of around 150 ~ 200 °C and over 300 °C . According to the unblocking temperature spectra, steps were selected under 270°C .

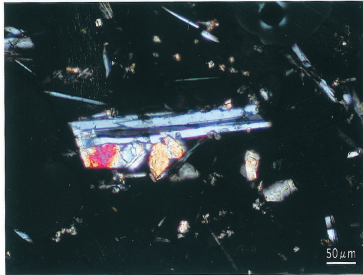
IRM acquisition curves:

IRM acquisition experiment was performed on the high density block by applying a pulse field. As shown in Fig.4, 300mT was the saturation field. The acquisition curve in every temperature was simple as compared with the deviating demagnetization curve.

Sample: H3-1

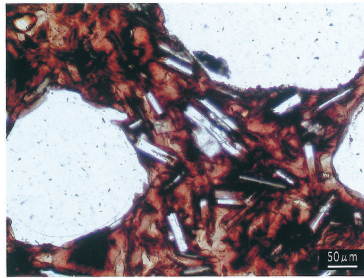


Plane-polarized light

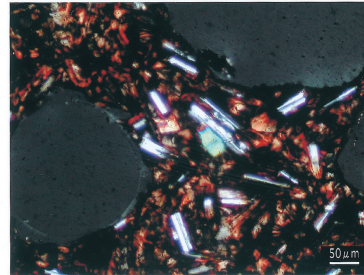


Crossed polars

Sample: H3-2

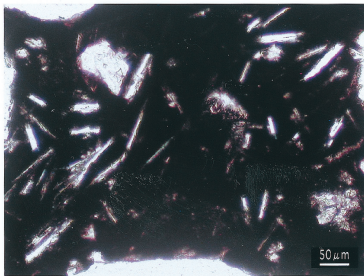


Plane-polarized light

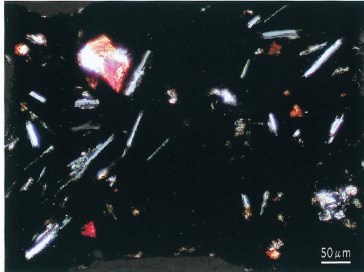


Crossed polars

Sample: H3-3

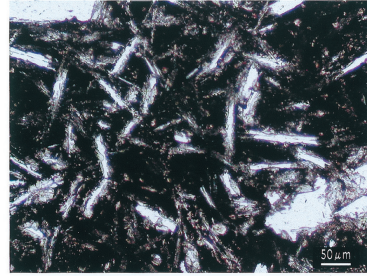


Plane-polarized light

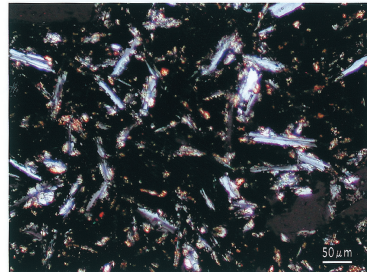


Crossed polars

Sample: H3-4



Plane-polarized light



Crossed polars

Fig. 2-2 Microscopic observation of RN98_H3-1 ~ H3-4

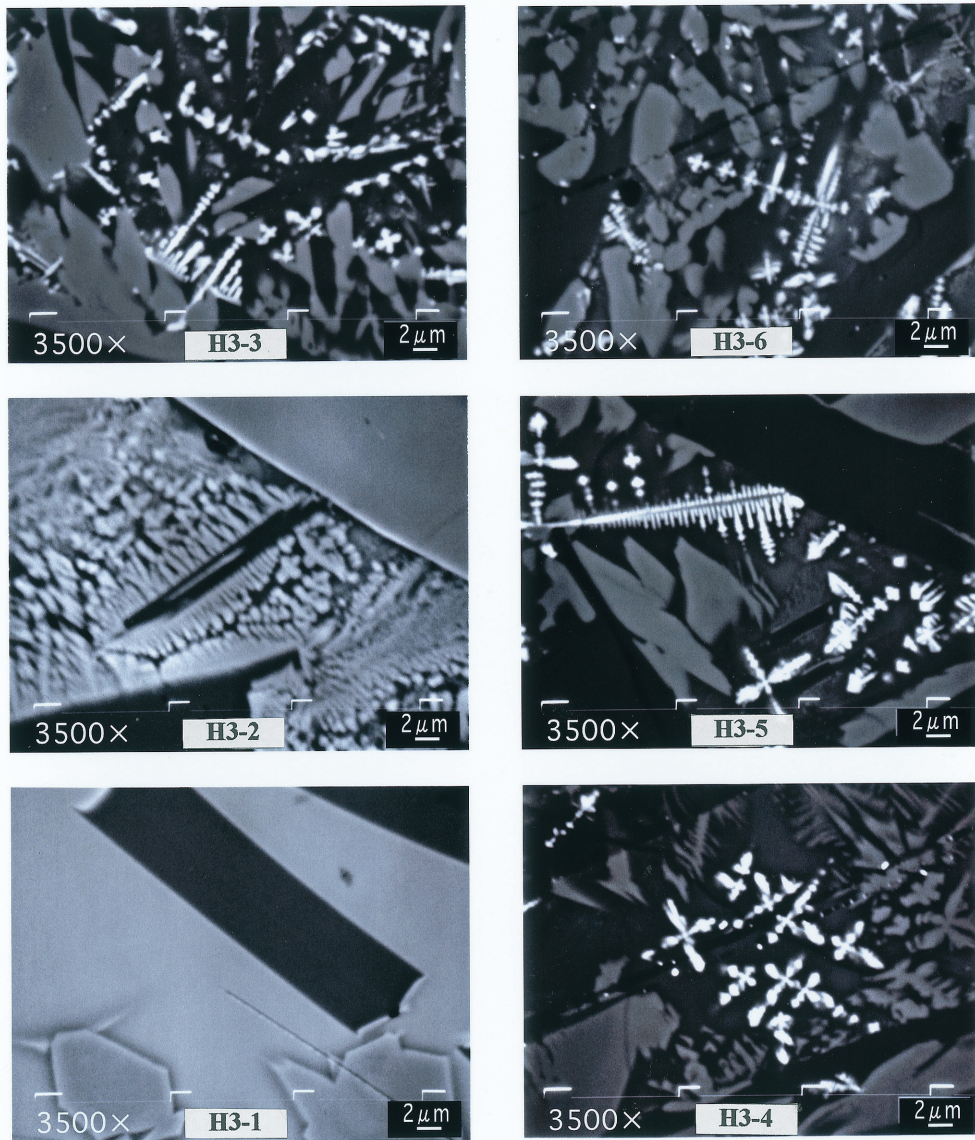


Fig. 2-3 BEI by scanning electron microscope of RN98_H3-1 ~ H3-6

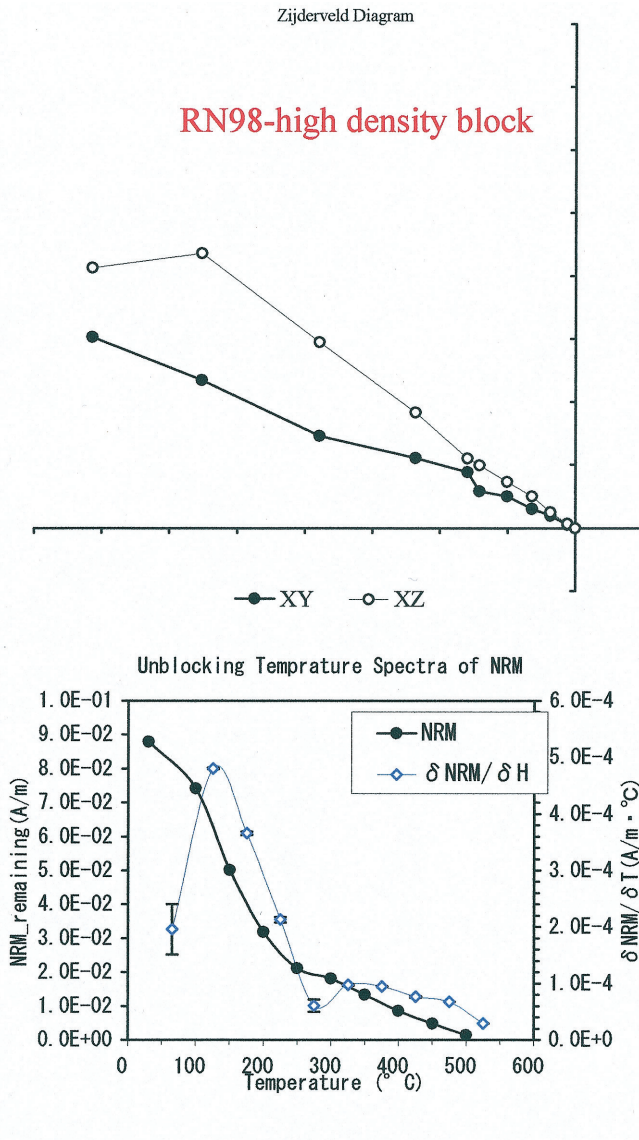


Fig. 3-1 Zijderveld diagram and unblocking temperature spectra of NRM on high density block

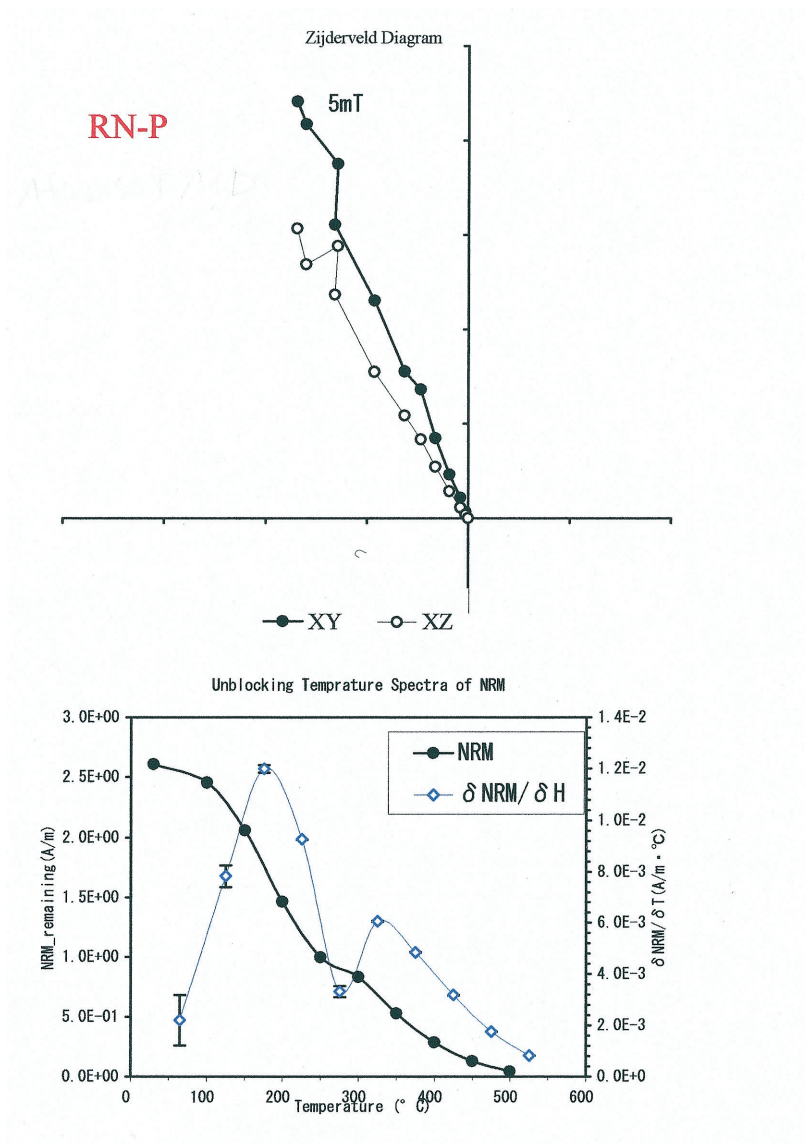


Fig. 3-2 Zijderveld diagram and unblocking temperature spectra of NRM on porous block

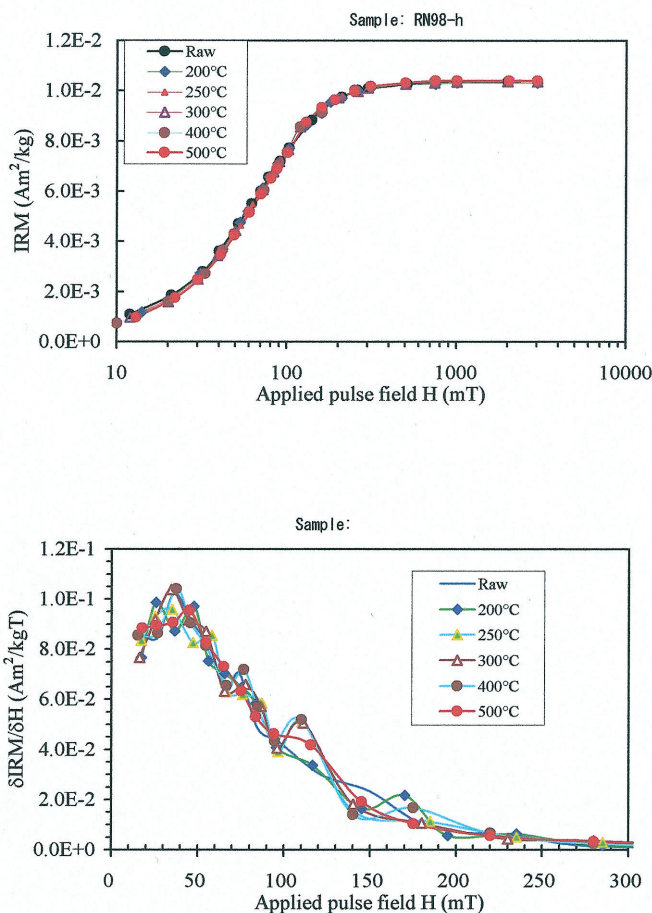


Fig. 4 IRM acquisition curve of high density block

Hysteresis parameters:

Hysteresis curves of H3-1 ~ H3-6 are shown in Fig.5. In Table 1, summary of the hysteresis parameters in H3-1 ~ H3-6 are listed, and the variation of H_c and H_{cr} in the specimens H3-1 ~ H3-6 was illustrated in Fig.6-1.

Plots of hysteresis parameters with files of titanomagnetites (Day diagram) are shown in Fig.6-2. In the Day diagram, H3-2 ~ H3-6 are filed in single domain region, while H3-1 is in pseudo-single domain region.

FORC diagram:

From the analysis of hysteresis properties, first-order reversal curves (FORCs) (Pike et

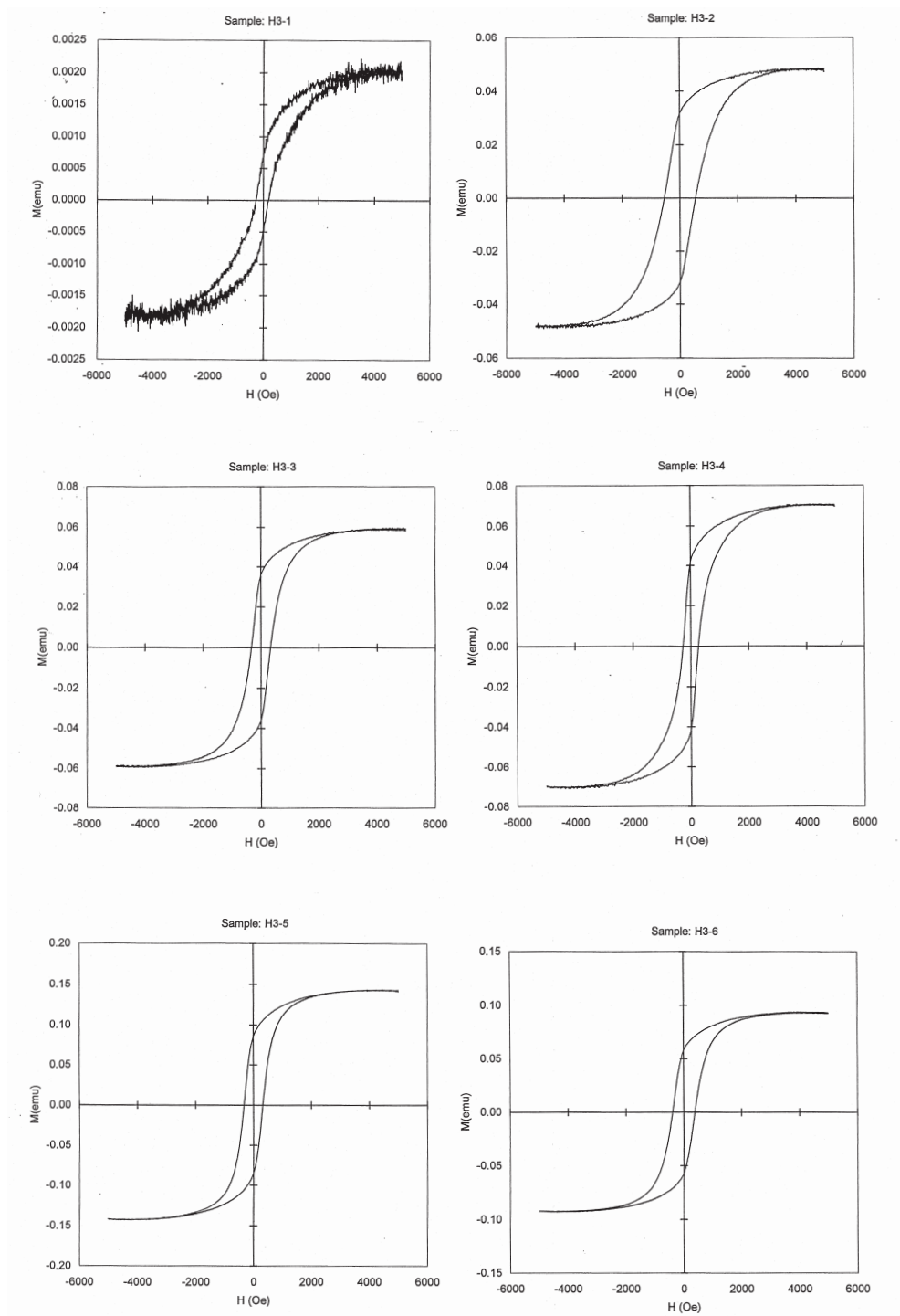
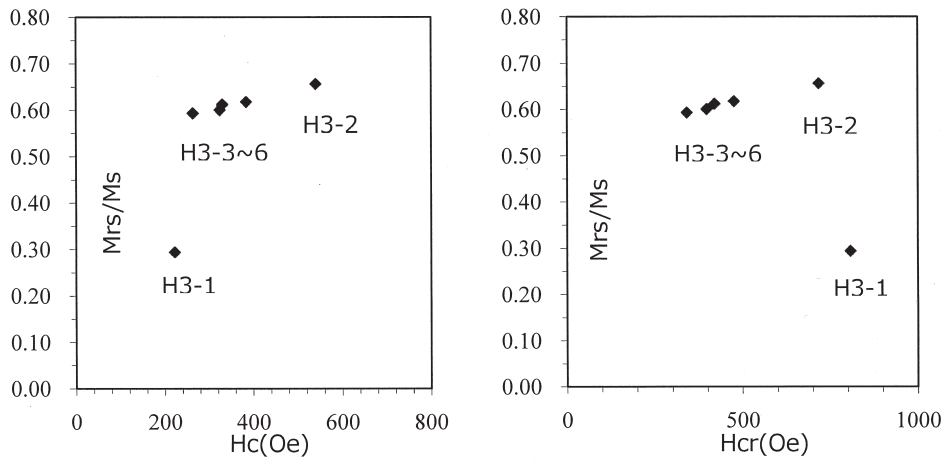


Fig. 5 Hysteresis curve of RN98_H3-1 ~ H3-6

Table 1 Hysteresis parameters of Reunion 1998 lava

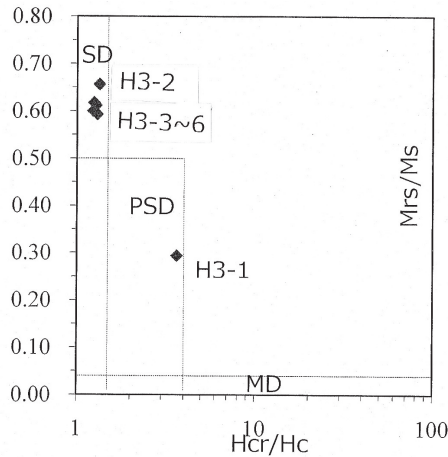
Hysteresis測定結果一覧表

順番	試料名	Hc(Oe)	Hcr	Msr(emu/g)	Ms(emu/g)	Hcr/Hc	Mrs/Ms
1	H3-1	222.7	806.8	1.881E-03	6.390E-03	3.62	0.294
2	H3-2	539.5	716.8	1.052E-01	1.602E-01	1.33	0.657
3	H3-3	329.9	419.4	1.331E-01	2.175E-01	1.27	0.612
4	H3-4	263.5	340.0	1.385E-01	2.333E-01	1.29	0.593
5	H3-5	324.1	396.7	2.841E-01	4.730E-01	1.22	0.601
6	H3-6	383.8	475.0	2.869E-01	4.644E-01	1.24	0.618



Hysteresis/パラメーター変化図

Fig. 6-1 Variation of Hc and Hcr in H3 specimens (vertical axis indicates Mrs/Ms)



チタノマグネタイト磁区分類図 Day et al. (1977)

Fig. 6-2 Plots of hysteresis parameters Single domain(SD),pseudo-SD(PSD) and multidomain(MD) files of titano-magnetites by Day et al.(1977) are also shown.

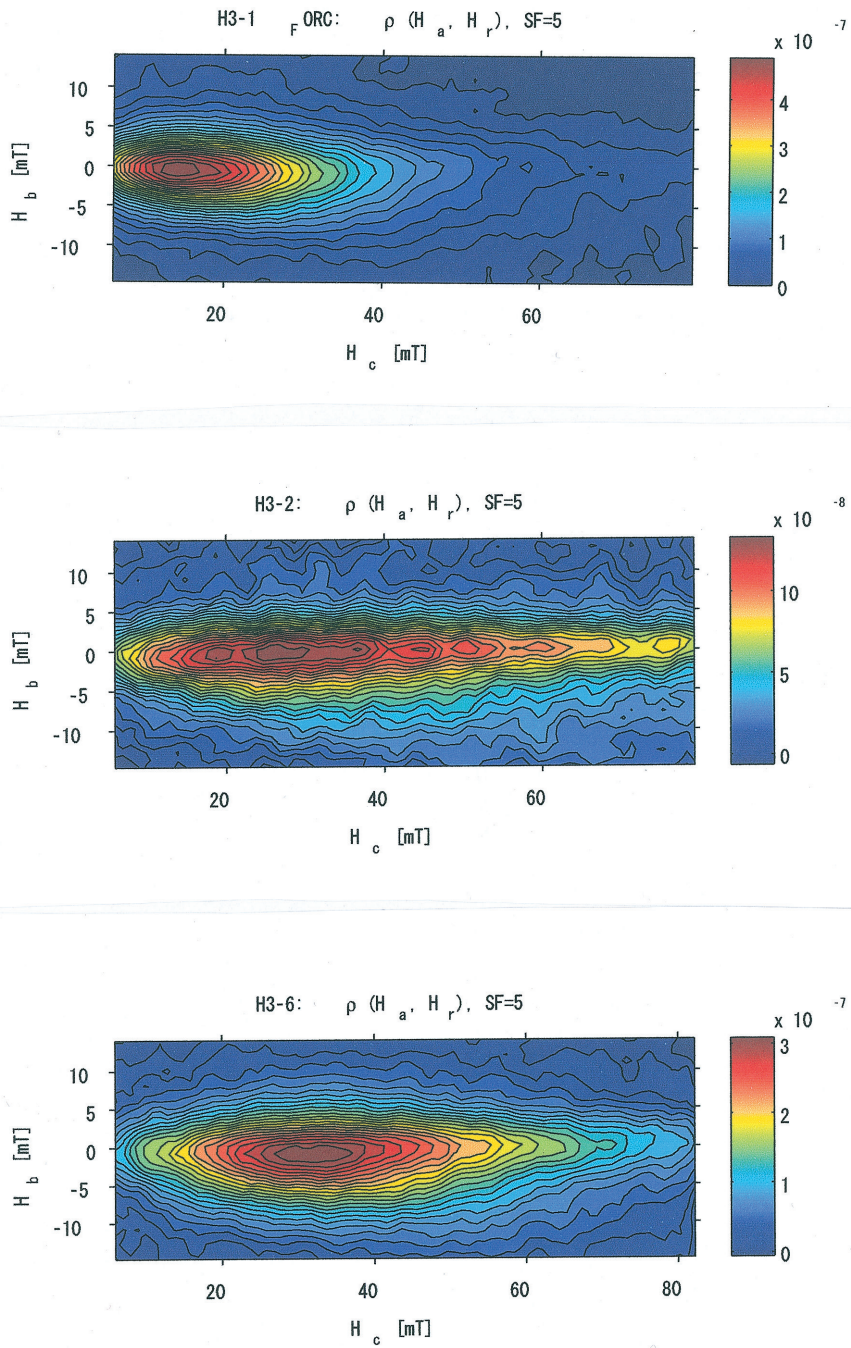


Fig. 7 FORC diagram of H3-1, H3-2, H3-6

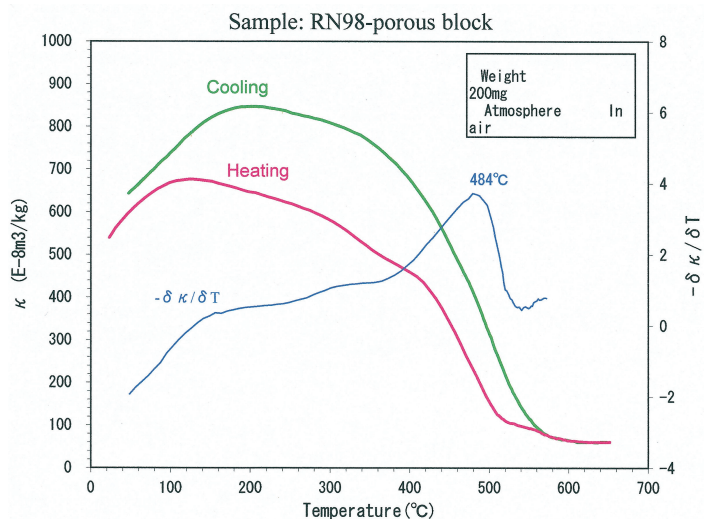


Fig. 8 Thermal analysis of initial susceptibility

al., 2001) are plotted in Fig.7. The high coercivity and the elongated minimal vertical spread of contours of H3-2 is the typical FORC figure of single domain titanomagnetite.

H3-1 filed in pseudo-single domain in Day diagram shows low maximum coercivity and relatively round figure compared with other two specimens filed in single domain area.

Thermal analysis of initial susceptibility:

Thermal analysis of initial susceptibility (κ) was conducted with Kappabridge susceptibility meter KLY-3S in air atmosphere to find out the magnetic phase change during laboratory heating. Only the specimen from porous block is analyzed as seen in Fig.8.

The significant phase change of the sample occurred at 484°C suggests the main magnetic mineral composition is close to magnetite.

3. Paleointensity experiment

The new method of paleointensity determination developed by Zheng was documented applicable by using the recent Unzen volcanic rocks (Ueno et al., 2008). The experiment procedure is introduced in detail in Ueno and Zheng (2010). Eleven samples were used: H1-1, H1-3 ~ H1-5, H2-9, H3-1 ~ 3-6. In Fig. 9-1-1, a diagram of unblocking temperature spectra of NRM & pTRM of specimen H1-1 for the 1st run to pick-up apparent paleointensity data is shown, and Fig. 9-1-2 shows the 2nd run for the correction of static-magnetic interaction between magnetic mineral grains. The results of the same experiment from other specimens are shown in from Fig. 9-2-1 to Fig. 9-11-2.

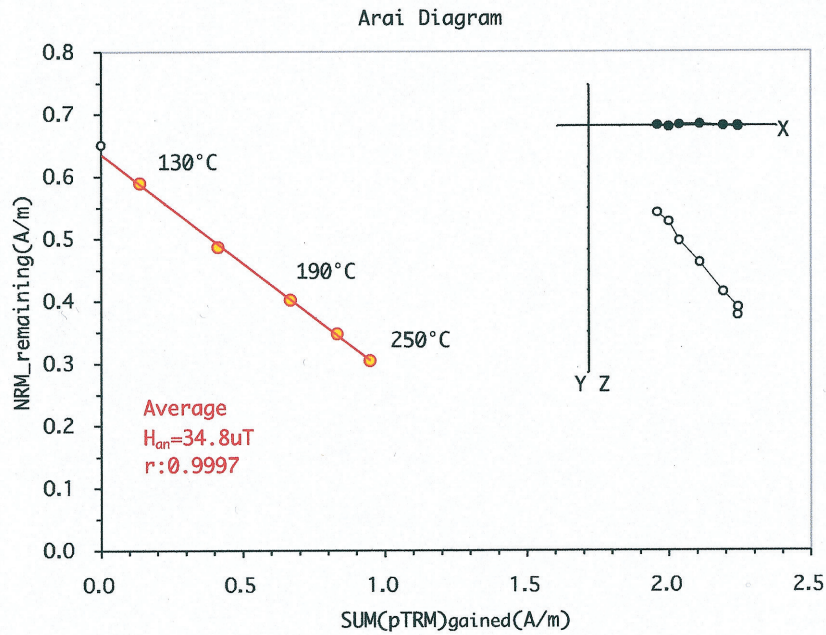
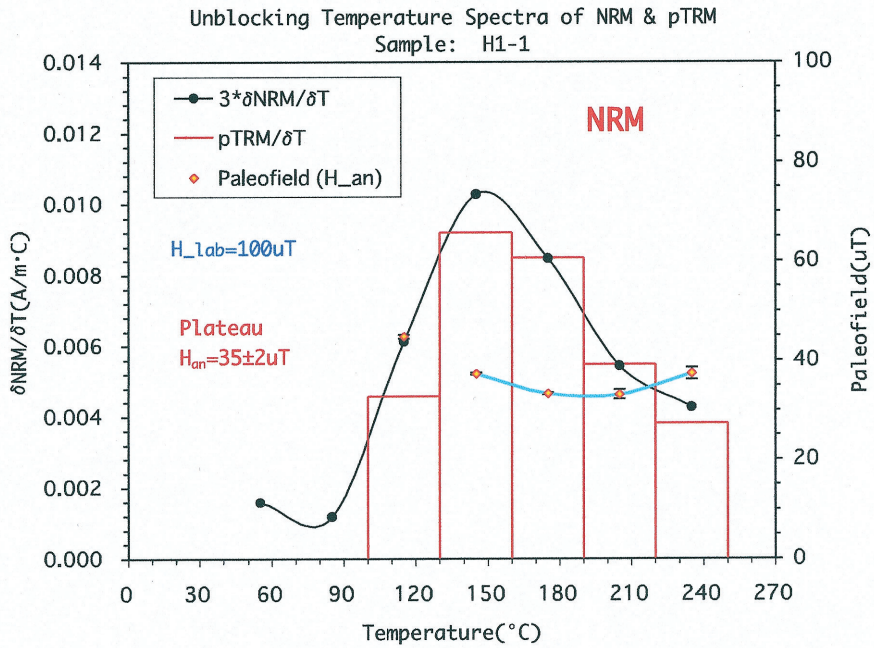


Fig. 9-1-1 Unblocking temperature spectra of NRM & pTRM of H1-1

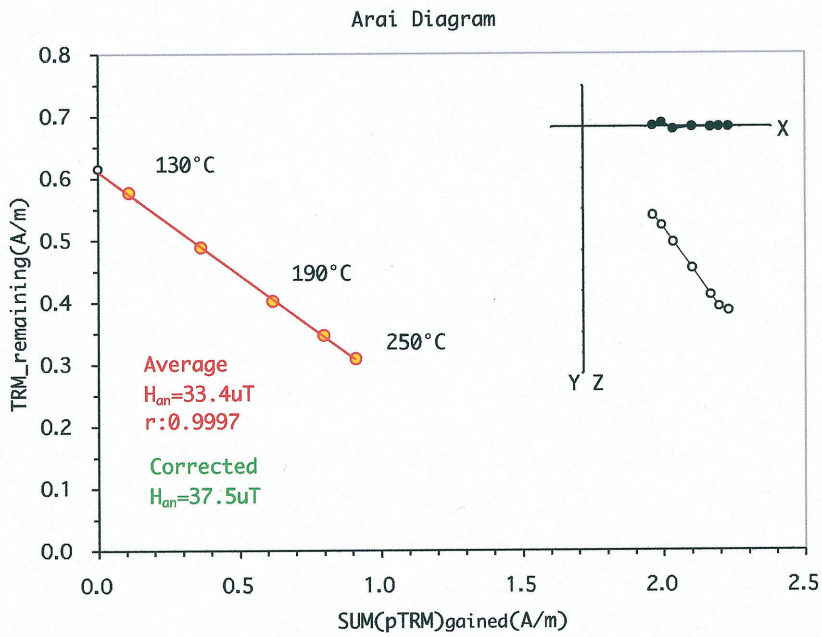
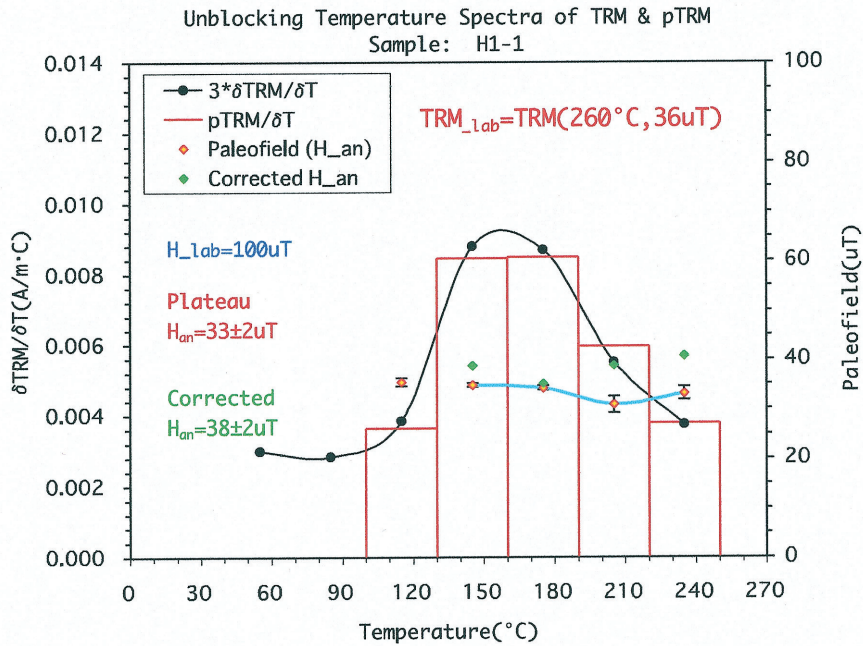


Fig. 9-1-2 Unblocking temperature spectra of TRM & pTRM of H1-1

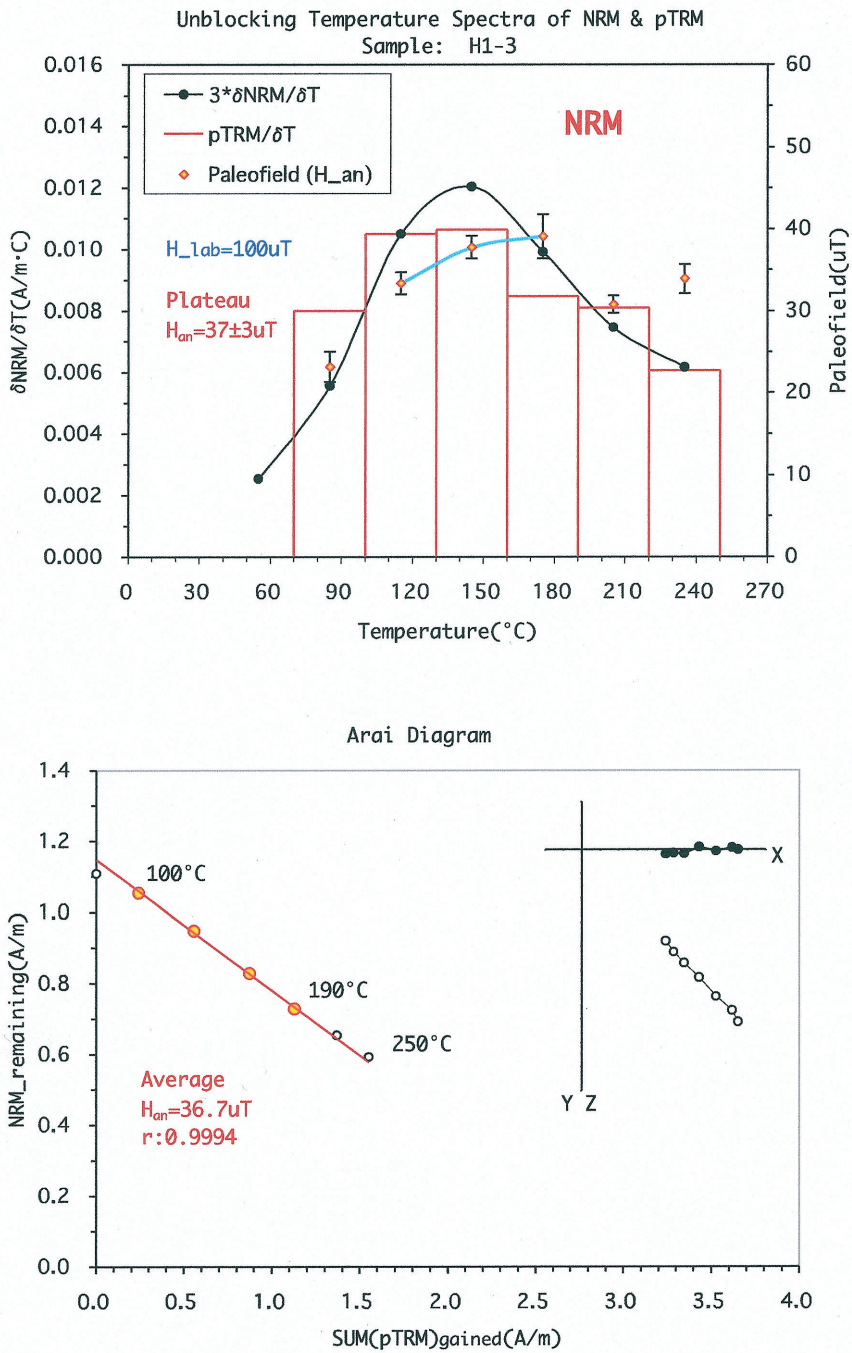


Fig. 9-2-1 Unblocking temperature spectra of NRM & pTRM of H1-3

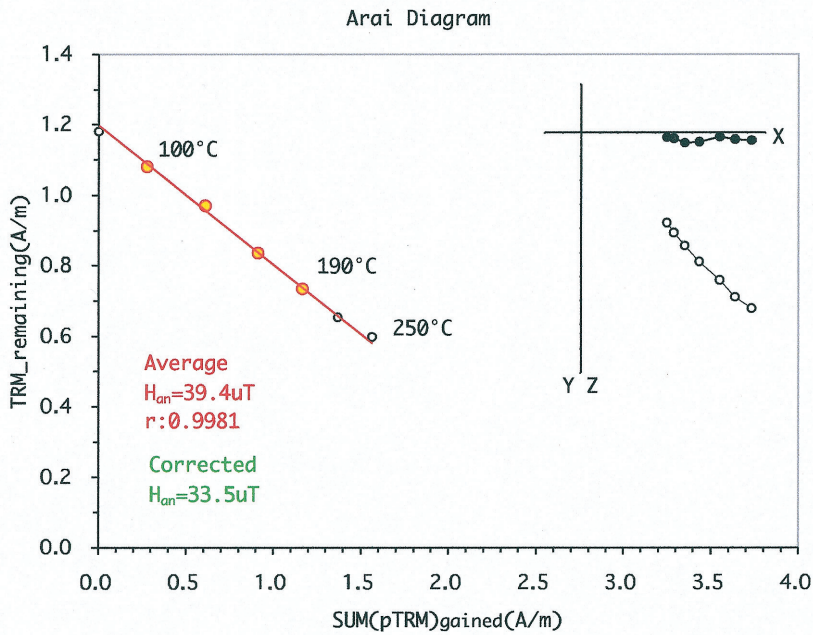
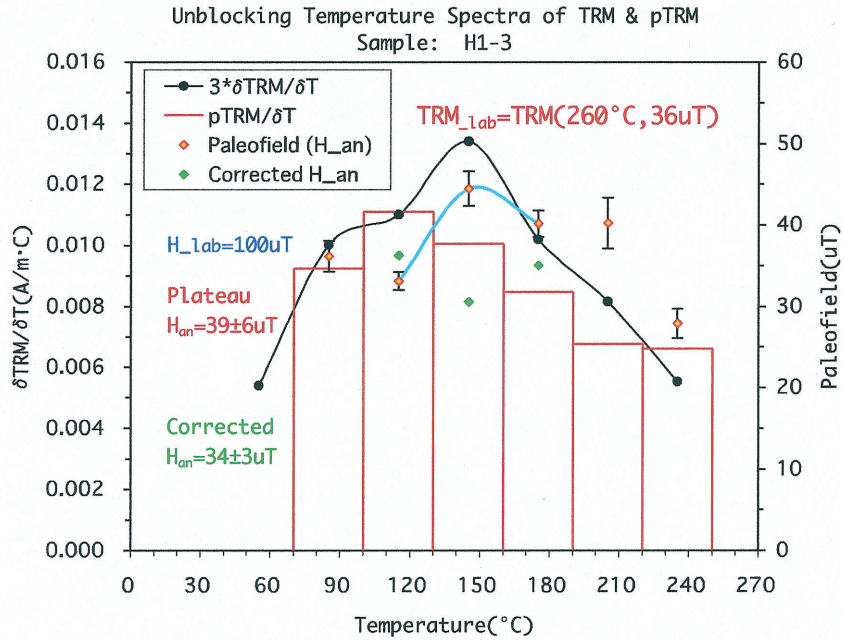


Fig. 9-2-2 Unlocking temperature spectra of TRM & pTRM of H1-3

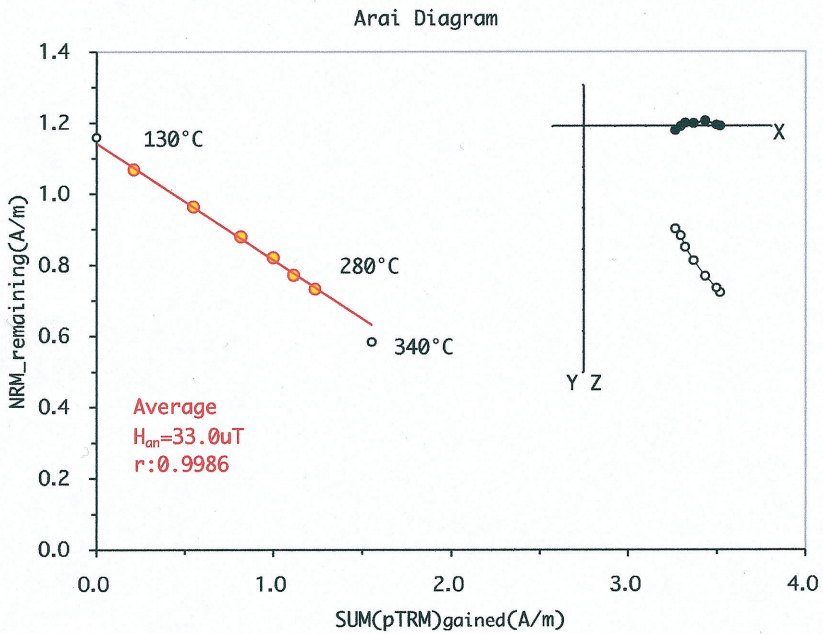
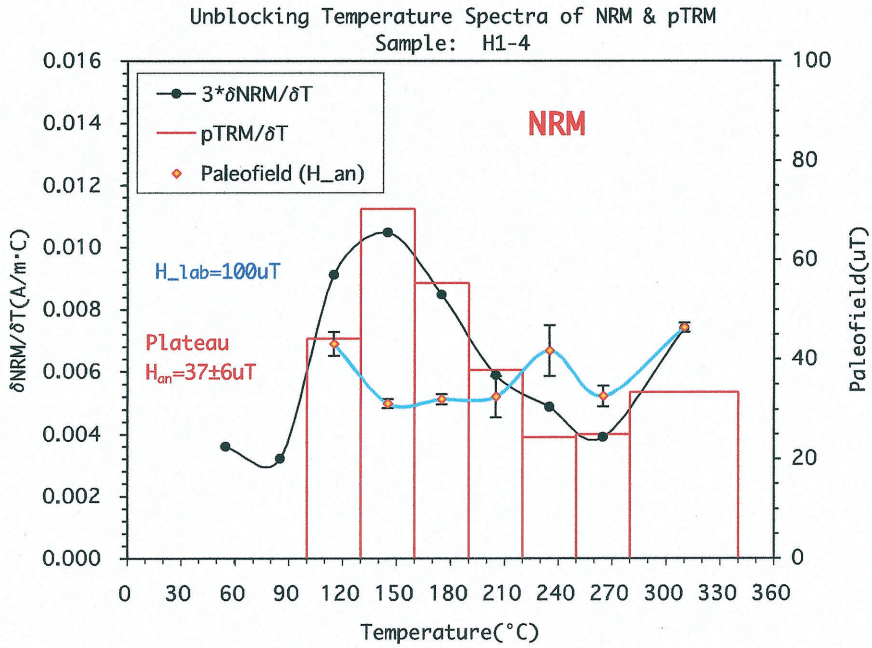


Fig. 9-3-1 Unlocking temperature spectra of NRM & pTRM of H1-4

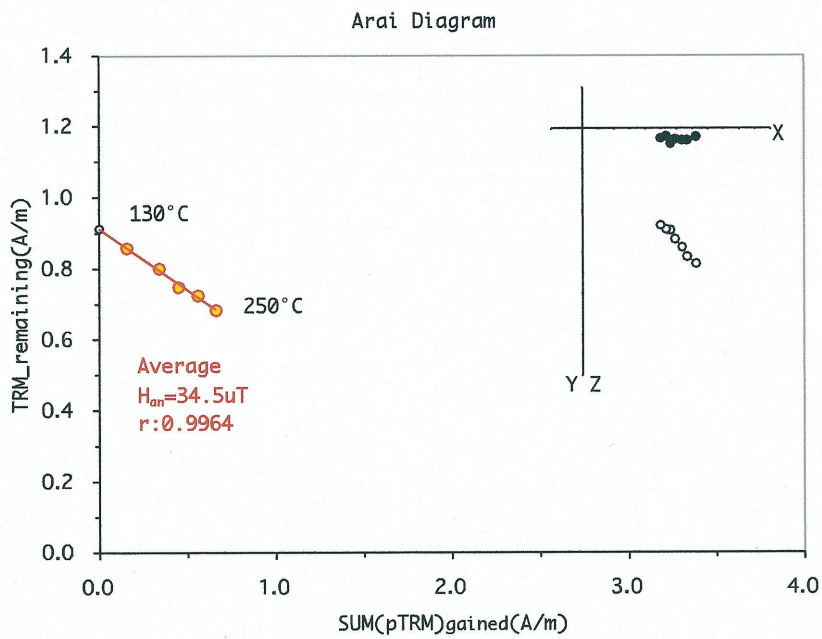
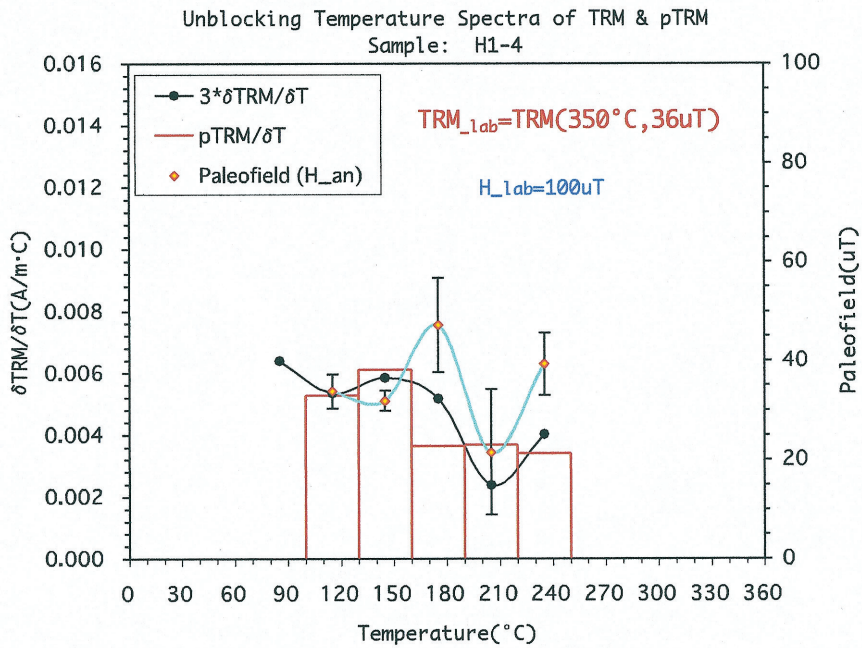


Fig. 9-3-2 Unblocking temperature spectra of TRM & pTRM of H1-4

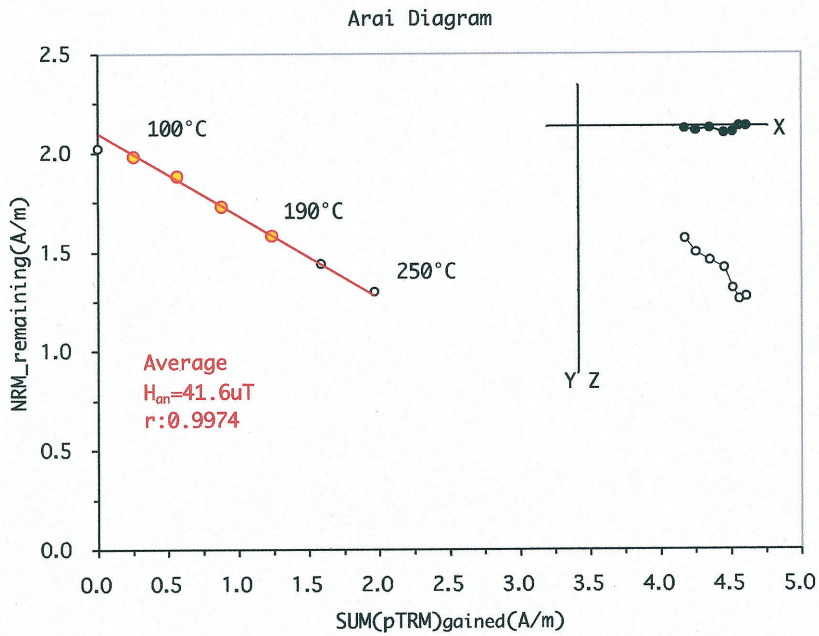
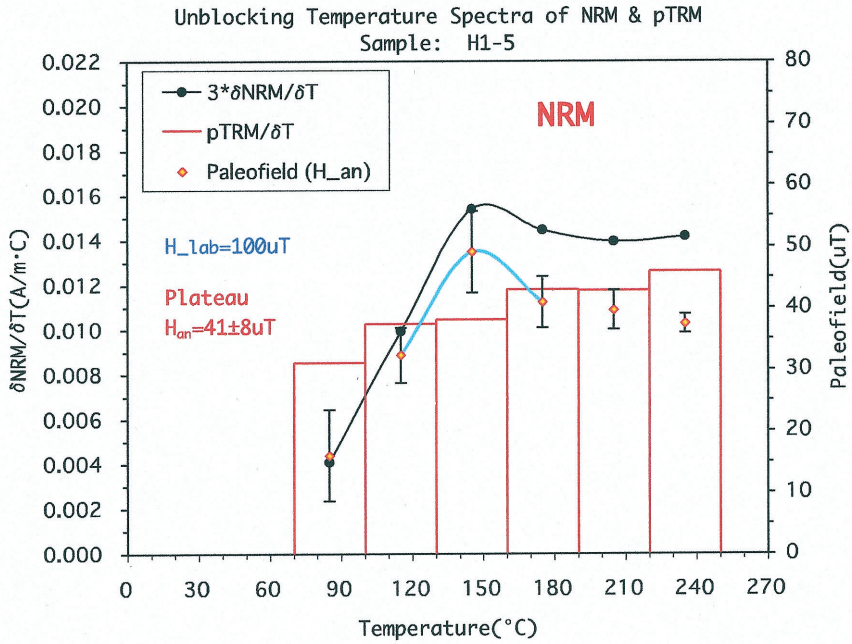


Fig. 9-4-1 Unblocking temperature spectra of NRM & pTRM of H1-5

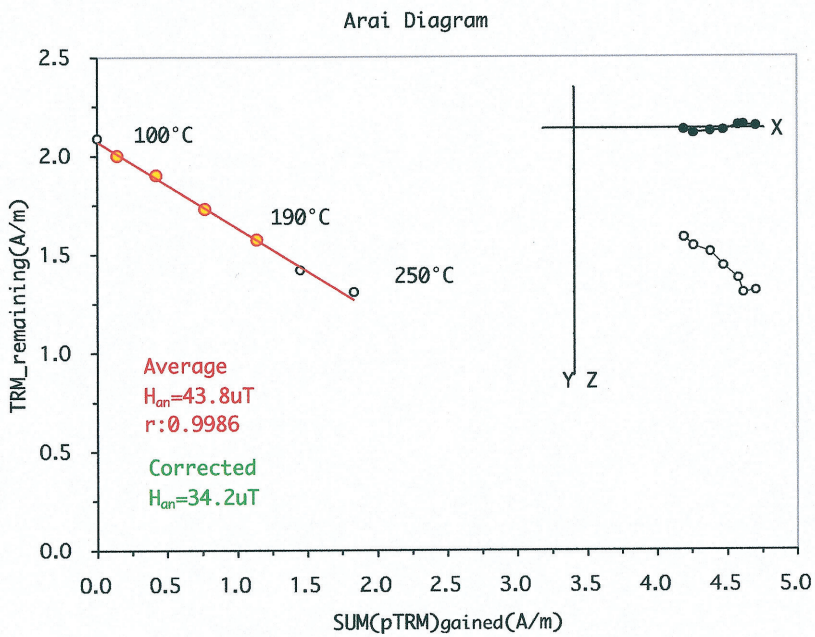
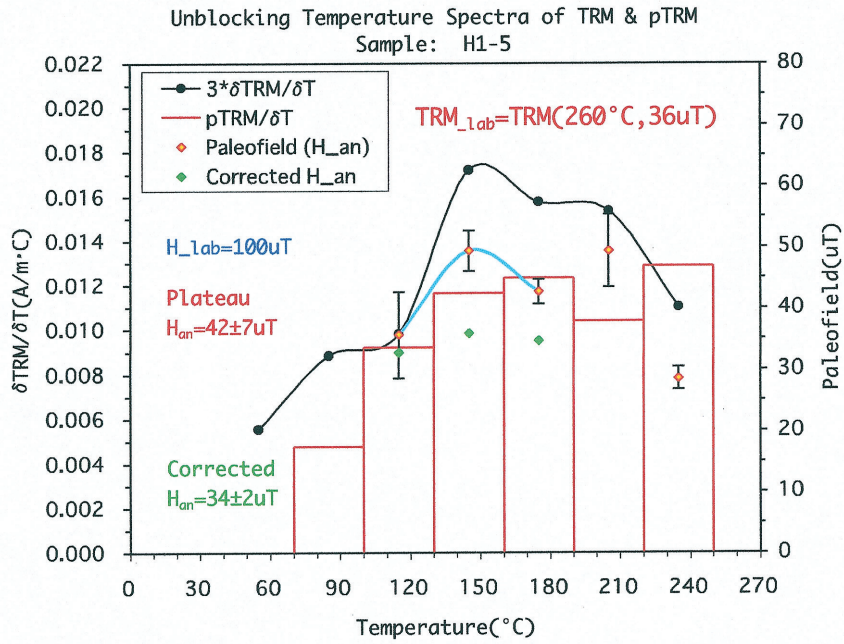


Fig. 9-4-2 Unblocking temperature spectra of TRM & pTRM of H1-5

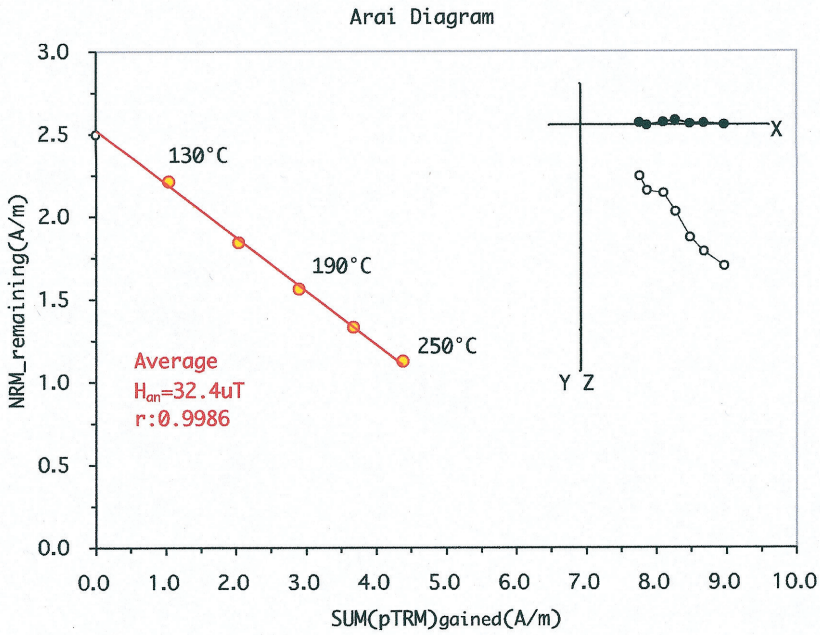
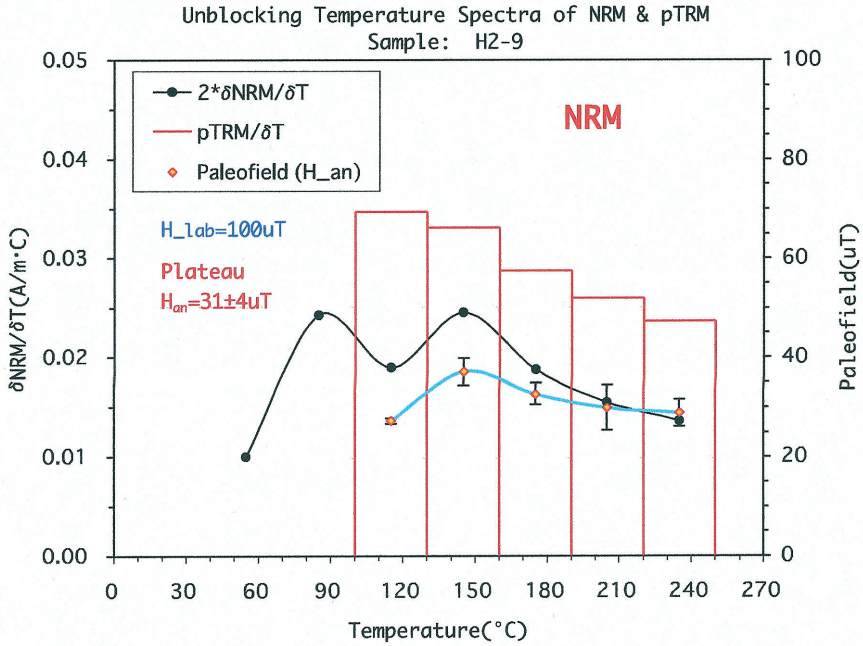


Fig. 9-5-1 Unblocking temperature spectra of NRM & pTRM of H2-9

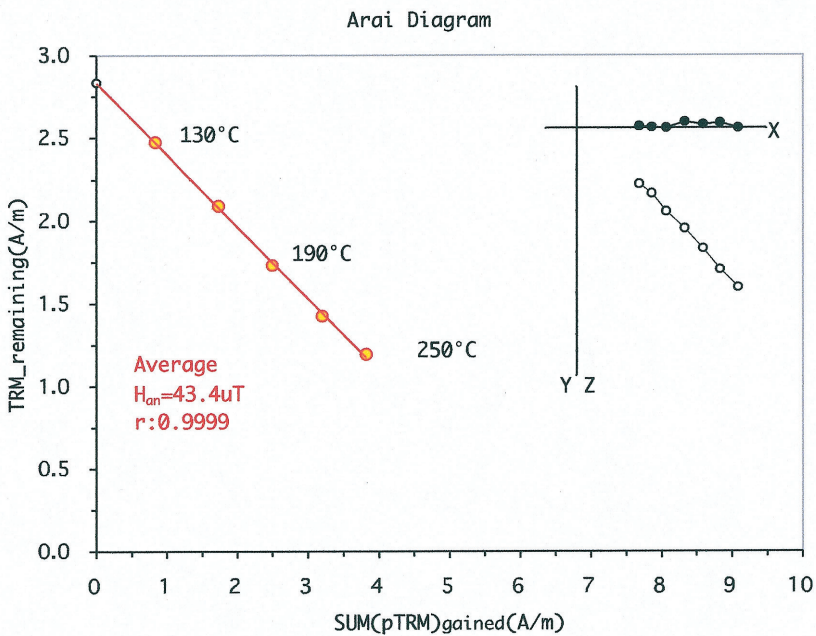
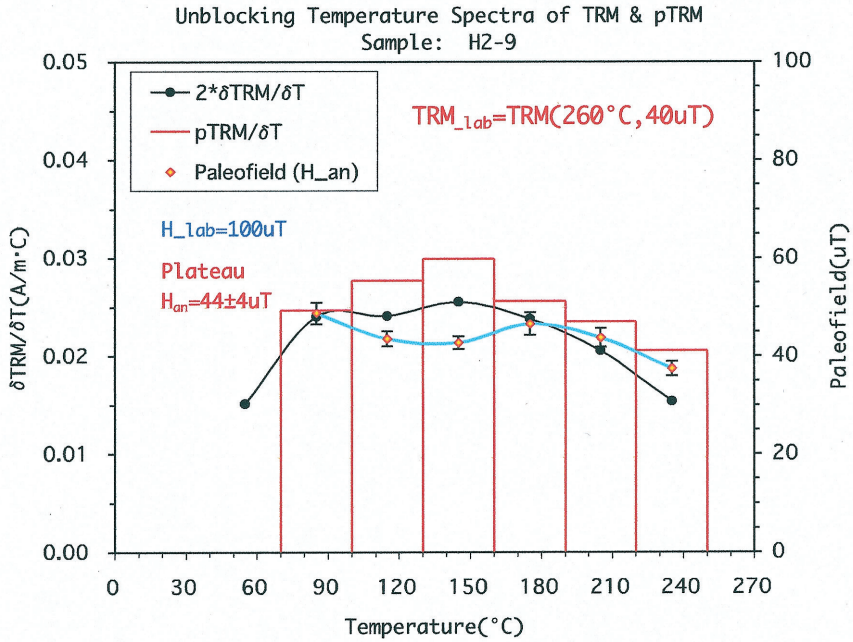


Fig. 9-5-2 Unblocking temperature spectra of TRM & pTRM of H2-9

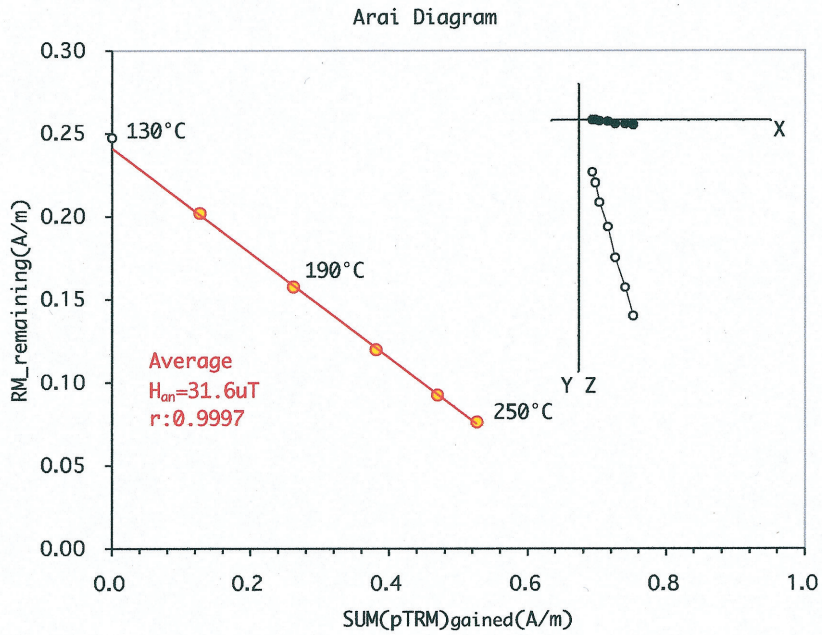
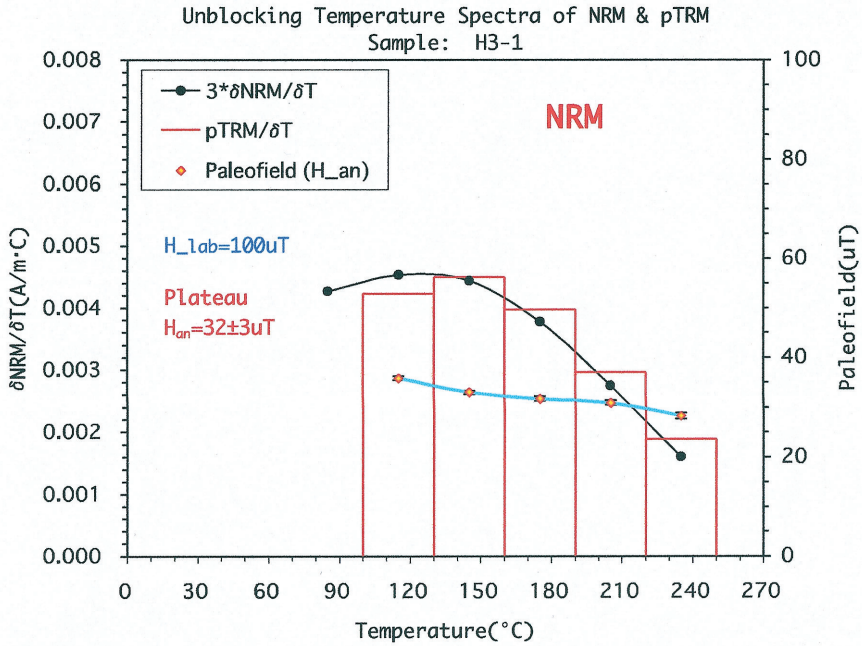


Fig. 9-6-1 Unlocking temperature spectra of NRM & pTRM of H3-1

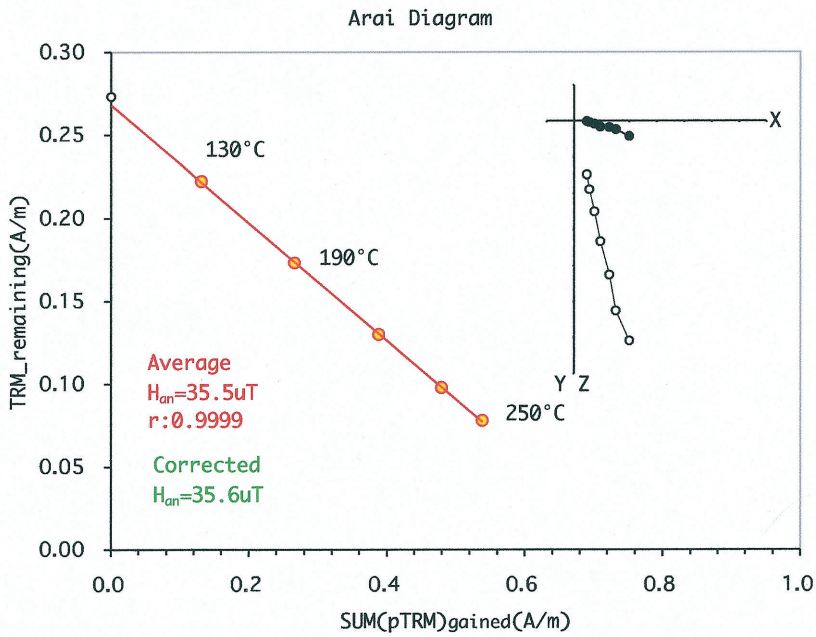
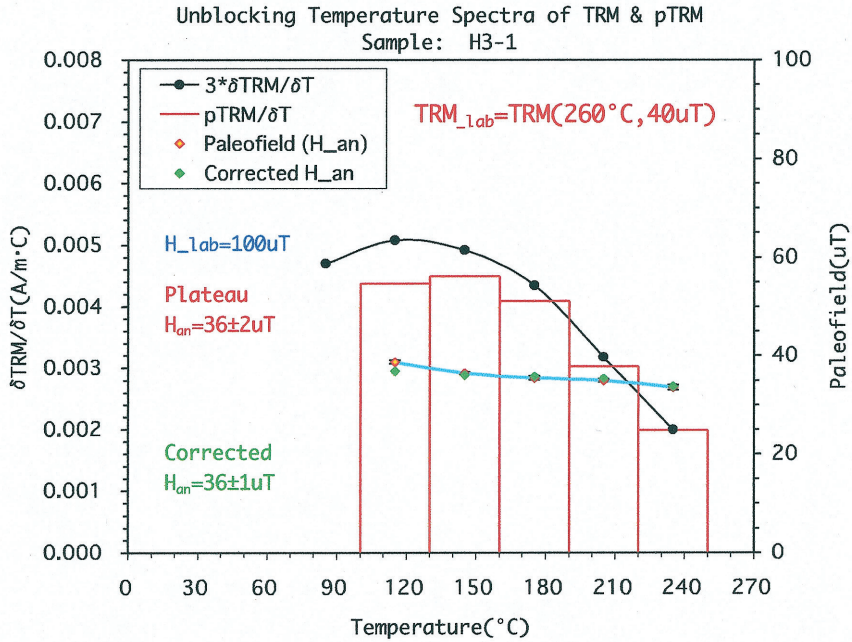


Fig. 9-6-2 Unblocking temperature spectra of TRM & pTRM of H3-1

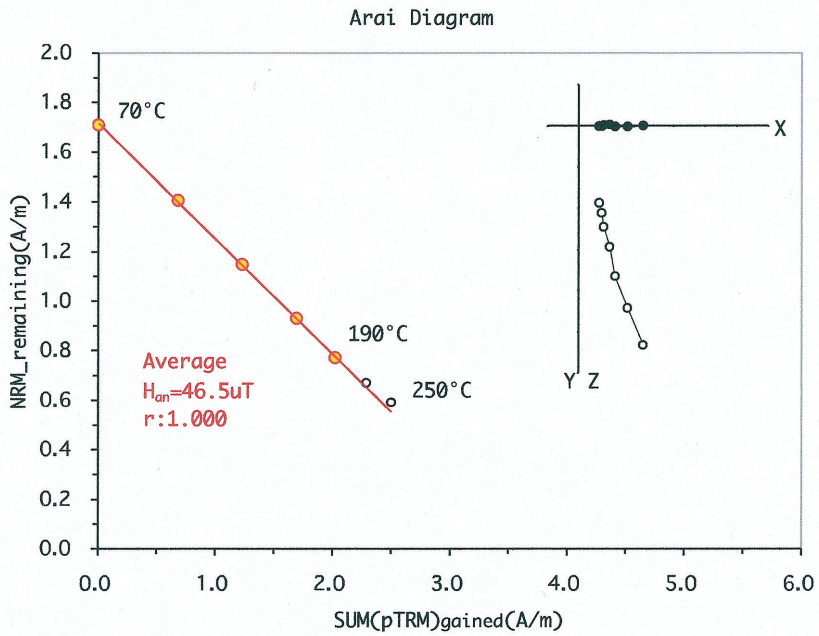
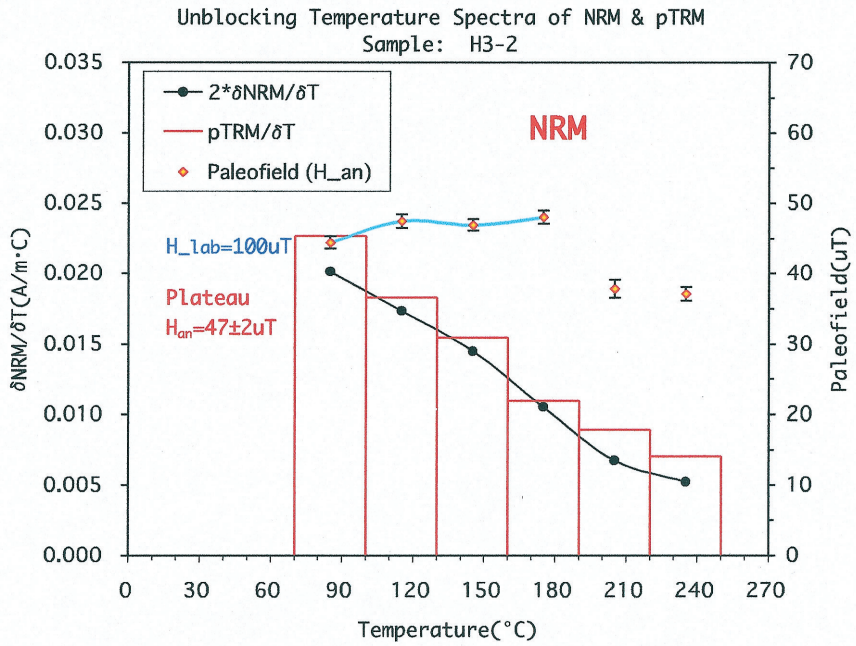


Fig. 9-7-1 Unblocking temperature spectra of NRM & pTRM of H3-2

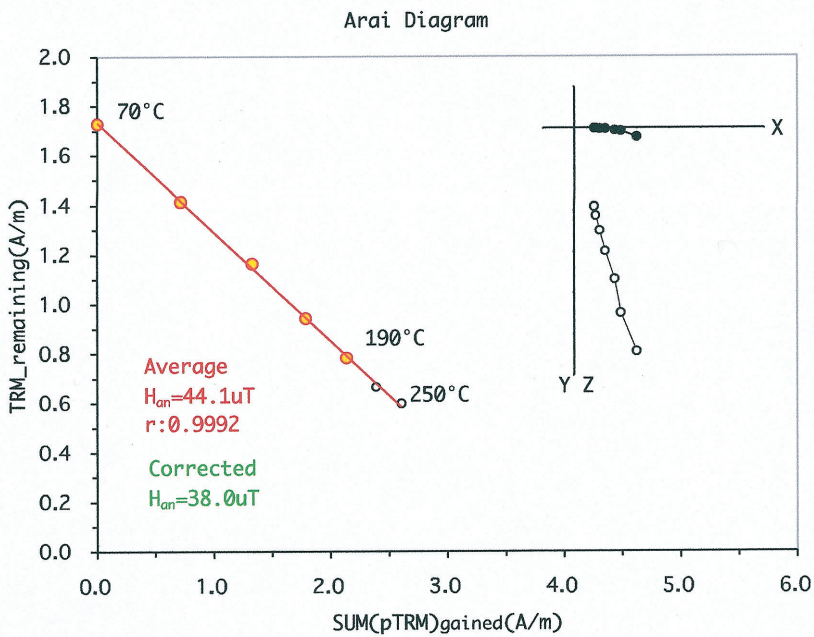
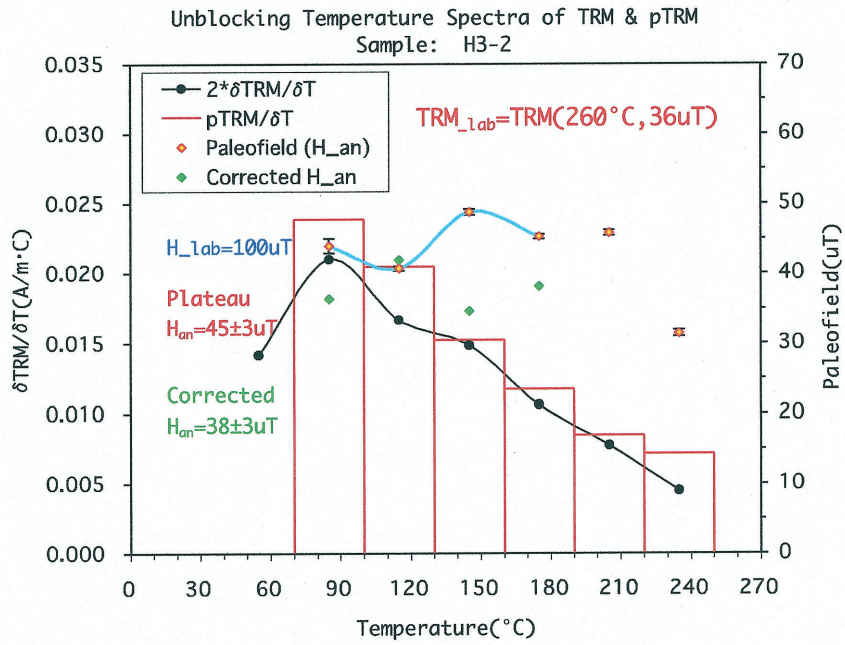


Fig. 9-7-2 Unblocking temperature spectra of TRM & pTRM of H3-2

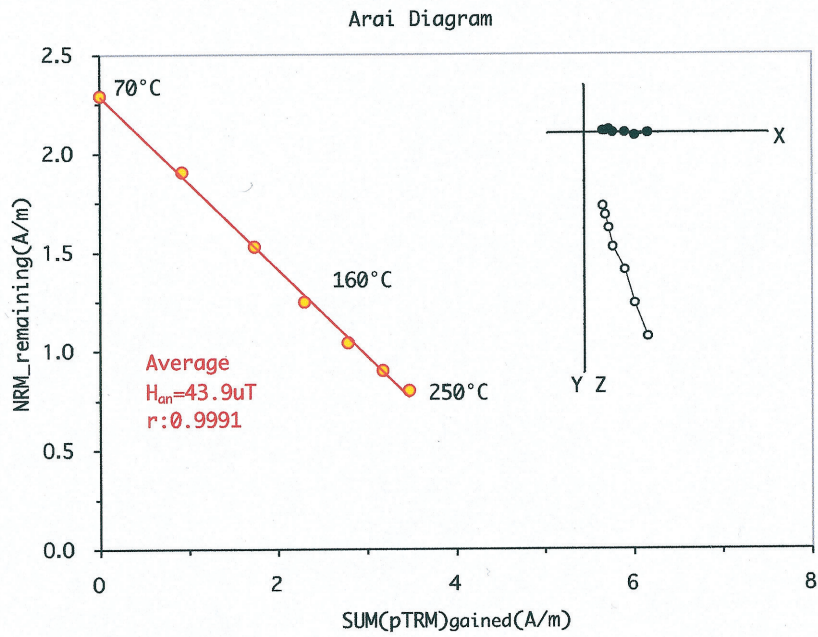
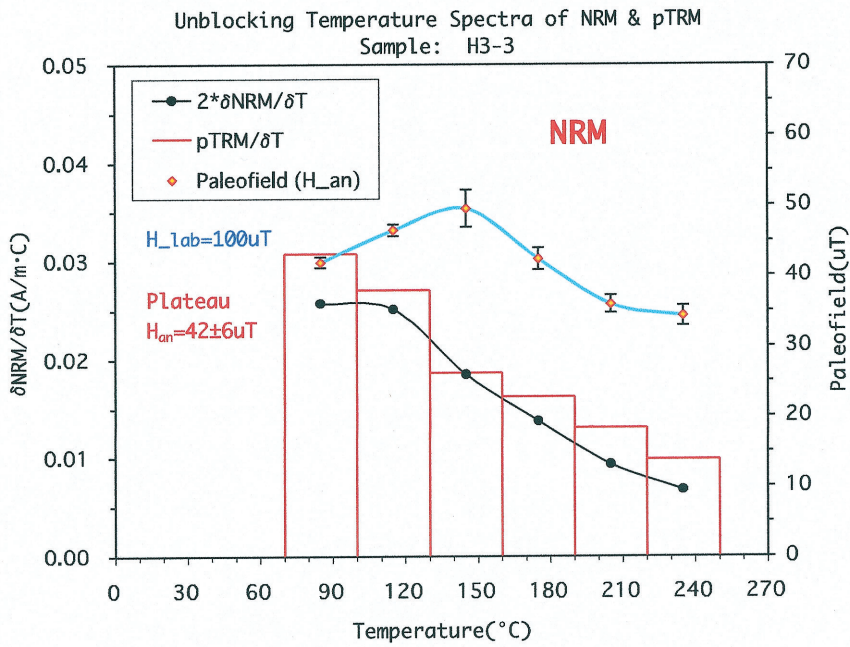


Fig. 9-8-1 Unlocking temperature spectra of NRM & pTRM of H3-3

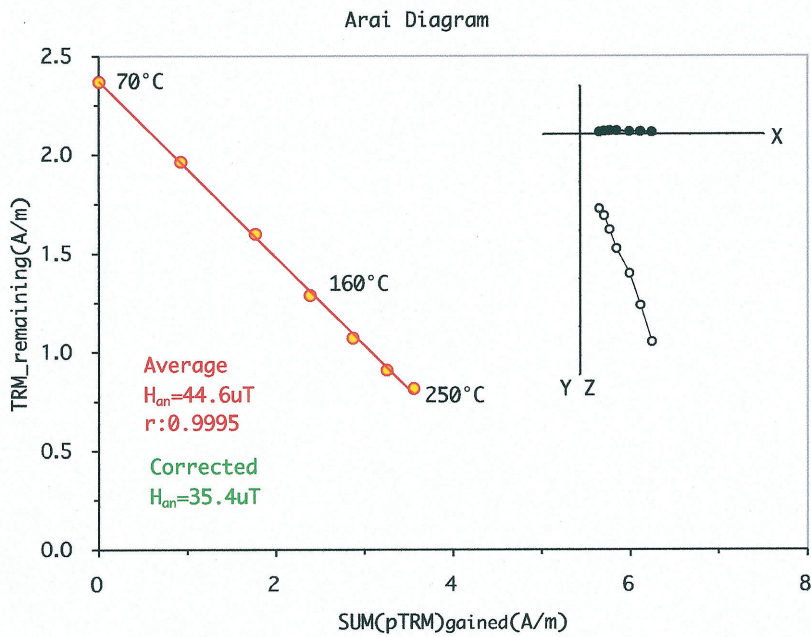
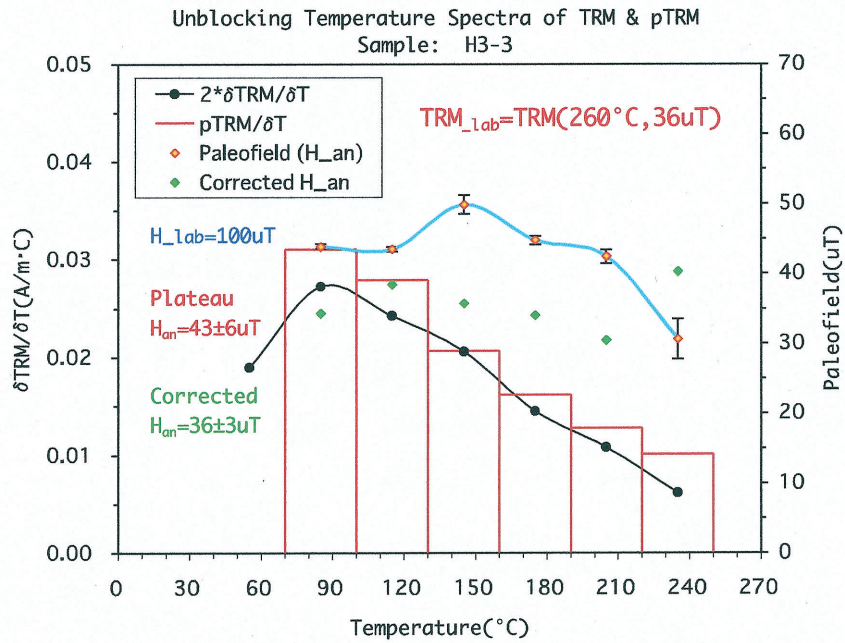


Fig. 9-8-2 Unblocking temperature spectra of TRM & pTRM of H3-3

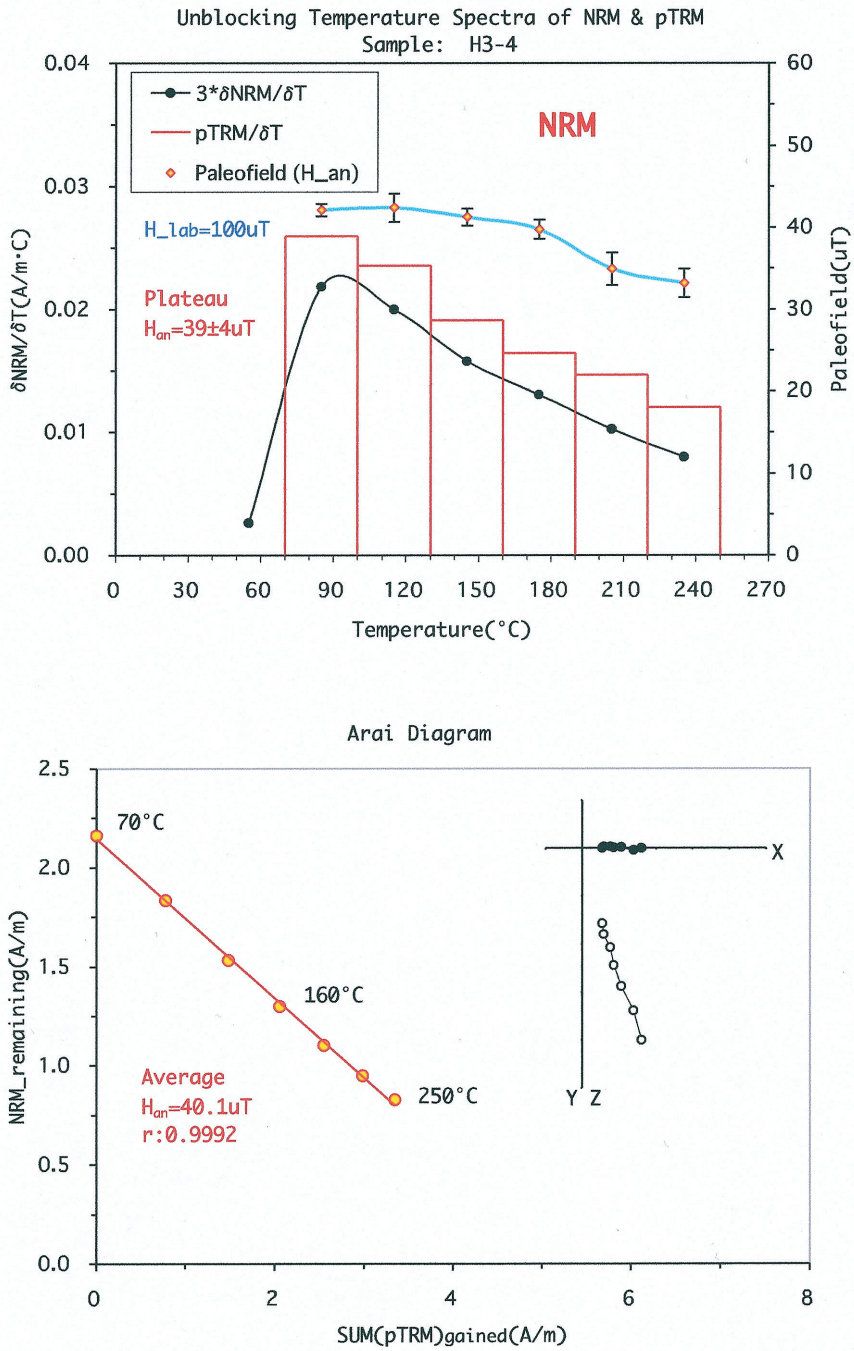


Fig. 9-9-1 Unlocking temperature spectra of NRM & pTRM of H3-4

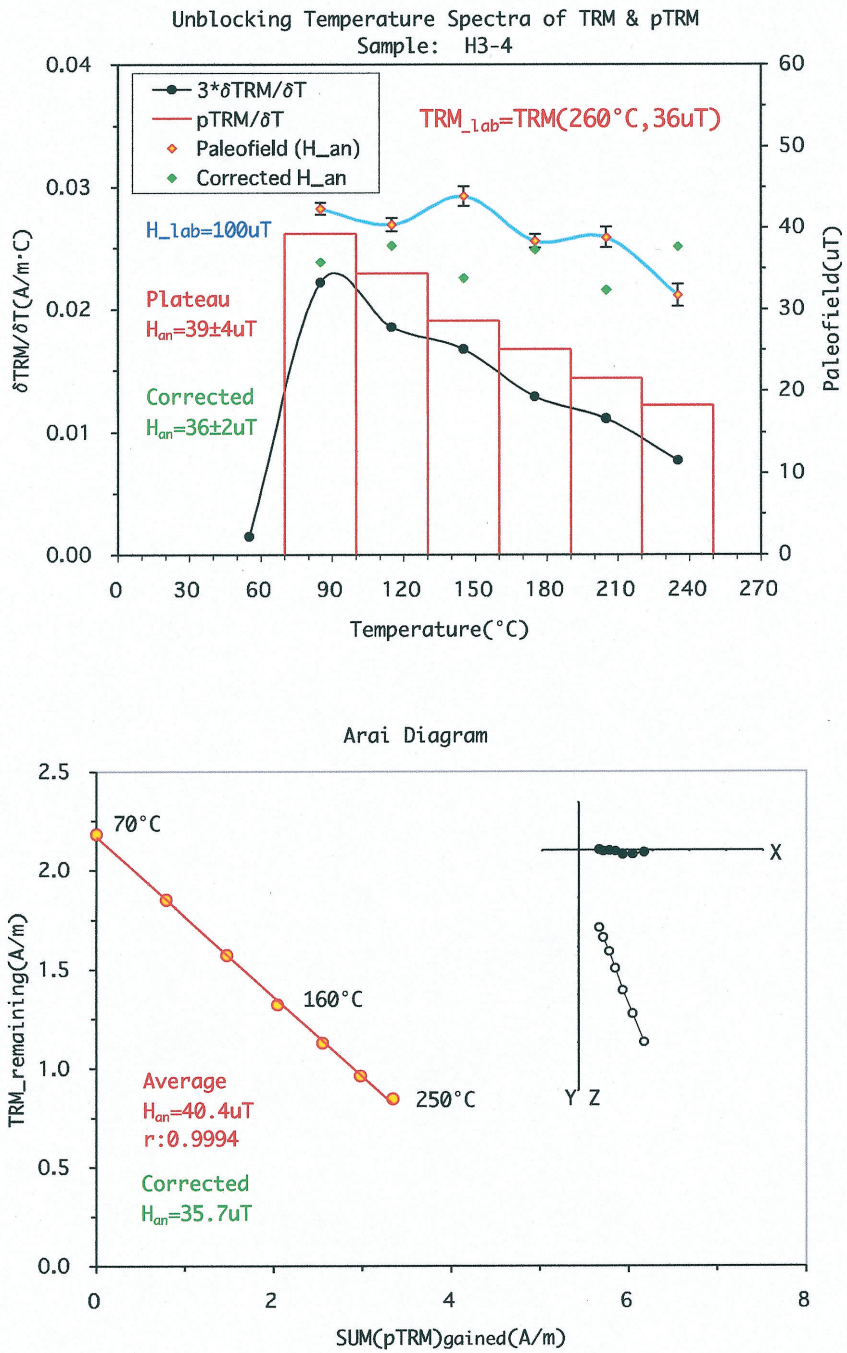


Fig. 9-9-2 Unblocking temperature spectra of TRM & pTRM of H3-4

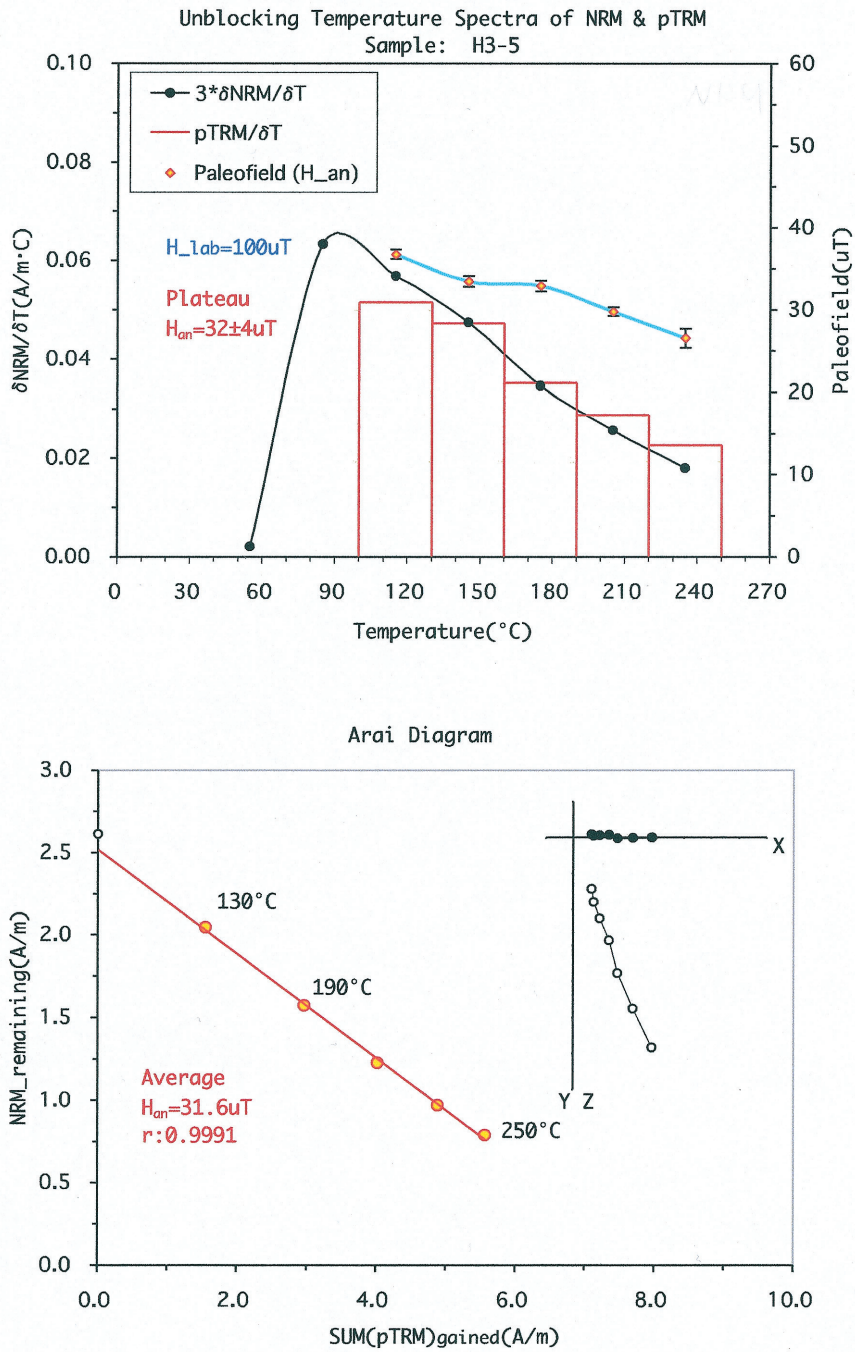


Fig. 9-10-1 Unblocking temperature spectra of NRM & pTRM of H3-5

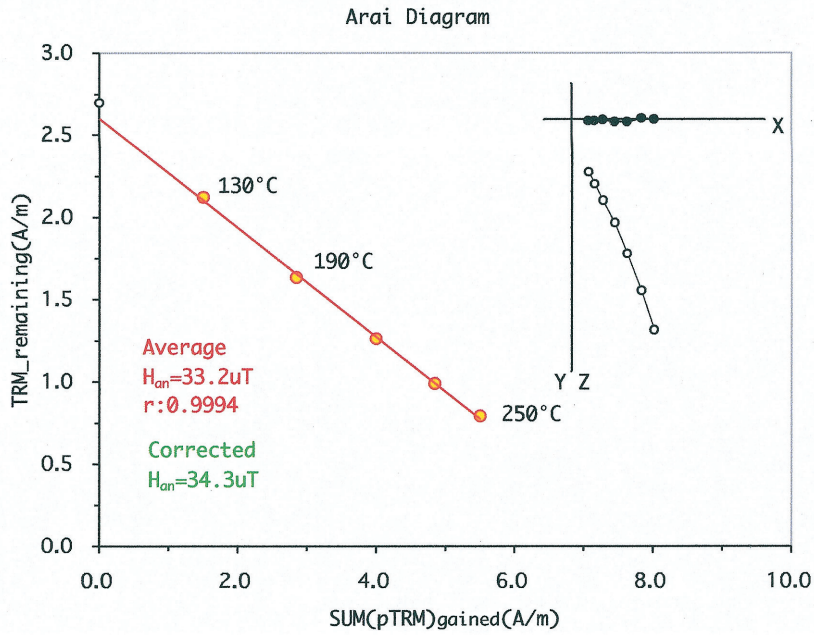
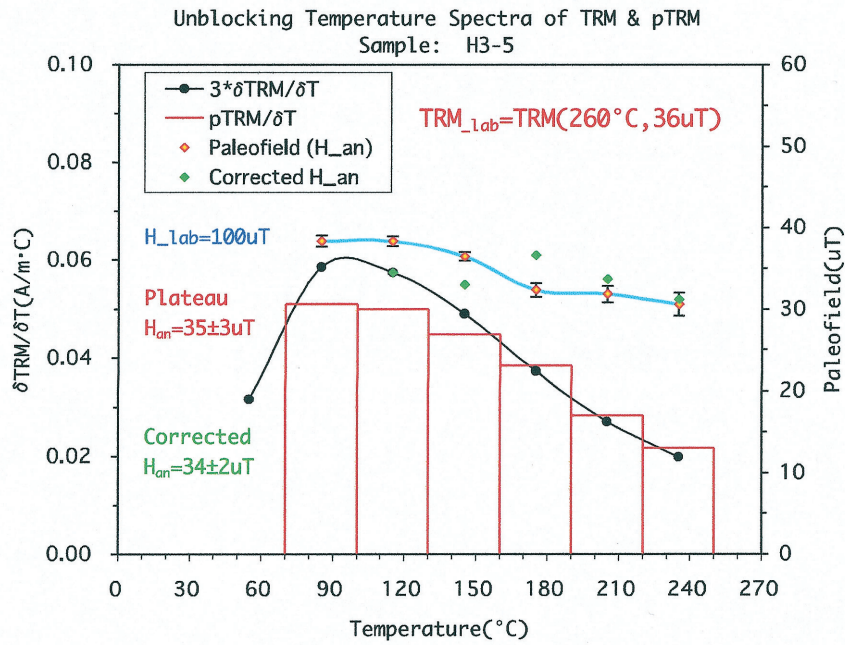


Fig. 9-10-2 Unblocking temperature spectra of TRM & pTRM of H3-5

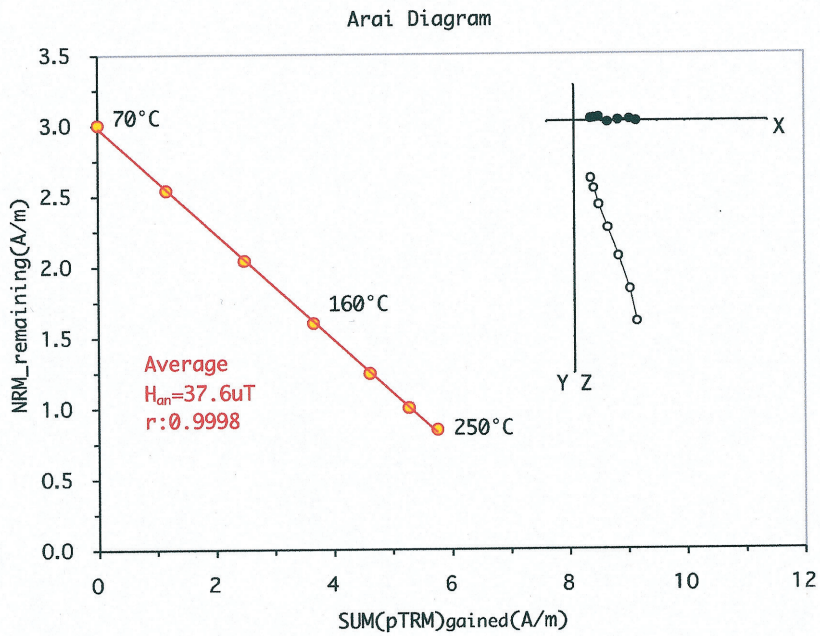
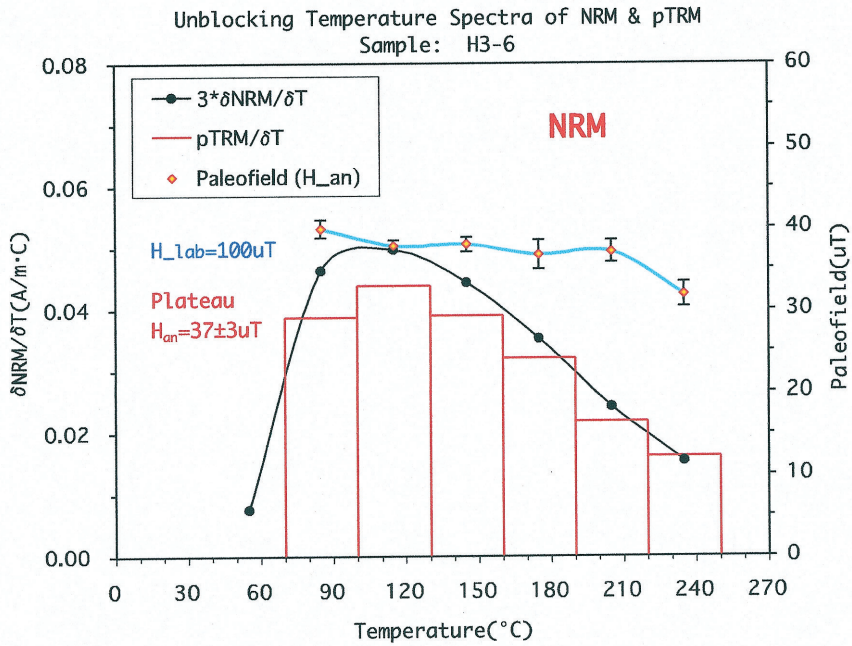


Fig. 9-11-1 Unblocking temperature spectra of NRM & pTRM of H3-6

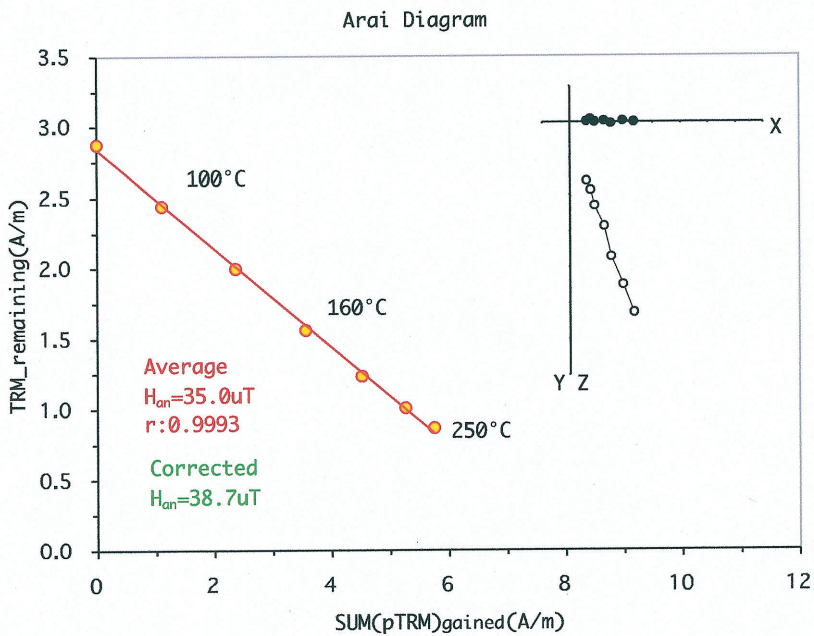
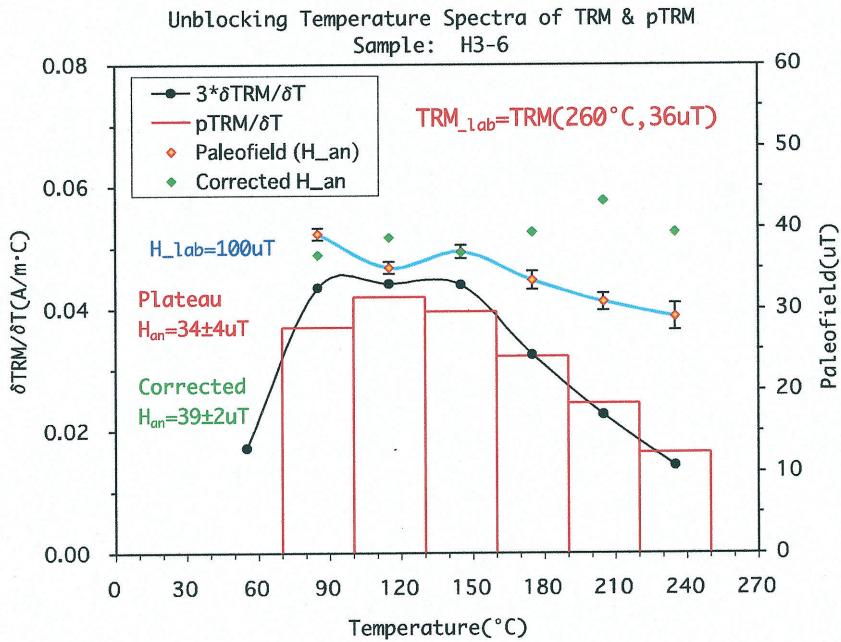


Fig. 9-11-2 Unlocking temperature spectra of TRM & pTRM of H3-6

Figure 10 shows histogram of paleointensity plateau data obtained from the 42 temperature intervals of 9 specimens from the most magnetic thermally stable lava. The upper panel diagram shows results of the differentiated Thelliers' method by using the data from NRM & pTRM spectra. The lower panel diagram represents the results of the new

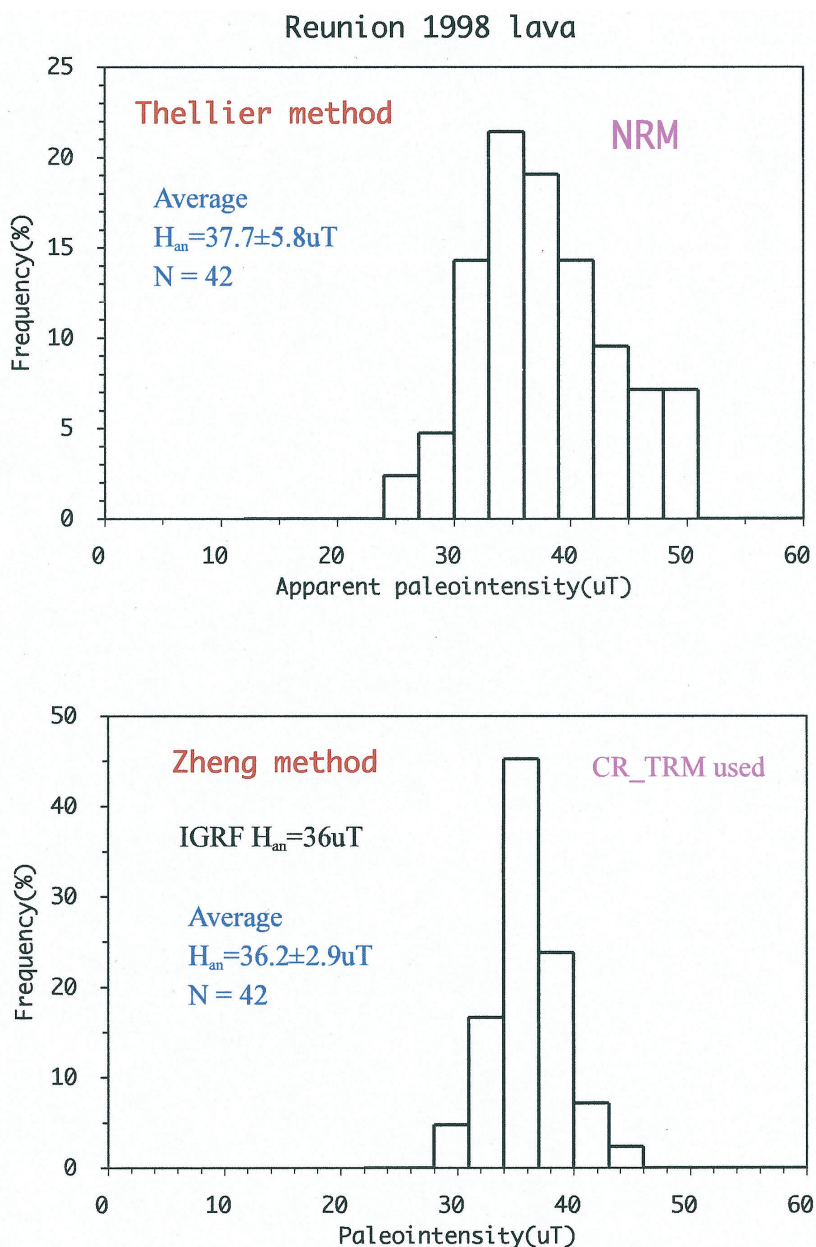


Fig. 10 Frequency distribution diagram of paleointensity on Reunion 1998 lava

Table 2 Summary of the intensity of Reunion 1998 lava

Table 2 Summary of paleomagnetic intensity results from Reunion 1998 basalt lava

Sample	Behaviour	AFD (mT)	H _{lab} (uT)	T _n (°C)	Range (°C)	N	SUM(pTRM ₂) / SUM(pTRM ₁)	δTRM / pTRM ₂	Paleo_intensity (uT)		NRM (A/m)	NRM(T _n) Reliability	
									Plateau	Corrected		NRM	NRM ₀
H1-1	-	-	36	260	130~250	4	0.989	0.92±0.05	35 ± 2	38 ± 2	2.70	44%	
H1-3	-	-	"	"	100~190	3	1.000	1.09±0.16	37 ± 3	34 ± 3	4.51	52%	
H1-5	-	-	"	"	100~190	3	1.019	1.18±0.19	41 ± 8	34 ± 2	7.98	64%	
H3-1	PSD-like	-	"	"	100~250	5	1.023	1.00±0.05	32 ± 3	36 ± 1	0.73	28%	
H3-2	SD-like	-	"	"	70~190	4	1.058	1.24±0.09	44 ± 2	38 ± 3	4.92	35%	
H3-3	"	-	"	"	70~250	6	1.025	1.18±0.18	42 ± 6	36 ± 3	6.97	36%	
H3-4	"	-	"	"	"	6	0.998	1.09±0.12	39 ± 4	36 ± 2	7.35	37%	
H3-5	"	-	"	"	100~250	5	0.996	0.94±0.09	32 ± 4	34 ± 2	12.11	24%	
H3-6	"	-	"	"	70~250	6	1.000	0.95±0.11	37 ± 3	39 ± 2	12.51	27%	
Mean (specimen)						9	1.01±0.02		37.7 ± 4.2	36.1 ± 1.9			E
Mean (Plateau)						42			37.7 ± 5.8	36.2 ± 2.9			
<i>Failed samples</i>													
H1-4	-	-	36	350	100~340	7	0.597	-	37 ± 6	-	2.09	47%	
H2-9	-	-	40	260	100~250	5	0.871	-	31 ± 4	-	8.87	37%	

Notes: N: Number of intervals from which apparent plateau paleofield was estimated, AFD: Strength of AF demagnetization pre-treatment,

H_{lab}: a laboratory field to produce TRM (a artificial "NRM") for the correction of magnetostatic interaction effect.

pTRM1: acquired during 1st RUN for "pick-up" apparent paleointensity, pTRM2: acquired during 2nd RUN for "correction" of

grain's interaction. NRM(T_n): remaining of NRM after thermal demagnetization at T_n step. Reliability: E (excellent), G (good), R (reference).

method of Zheng after using the spectra of TRM and pTRM for correction. The mean of 42 plateau data is calculated to $36.2 \pm 2.9 \mu\text{T}$ for Zheng's method and $37.7 \pm 5.8 \mu\text{T}$ for Thelliers' method; and mean of 9 specimens is $36.1 \pm 1.9 \mu\text{T}$ and $37.7 \pm 4.2 \mu\text{T}$ for Zheng's and Thelliers' respectively. The Zheng's data set is much smaller in dispersion than the differential Thelliers' method.

Summary of paleomagnetic intensity results from the Reunion 1998 lava is compiled in Table 2.

One sample from the high density block was applied to Shaw's method, and $31 \mu\text{T}$ was obtained as shown in Fig.11.

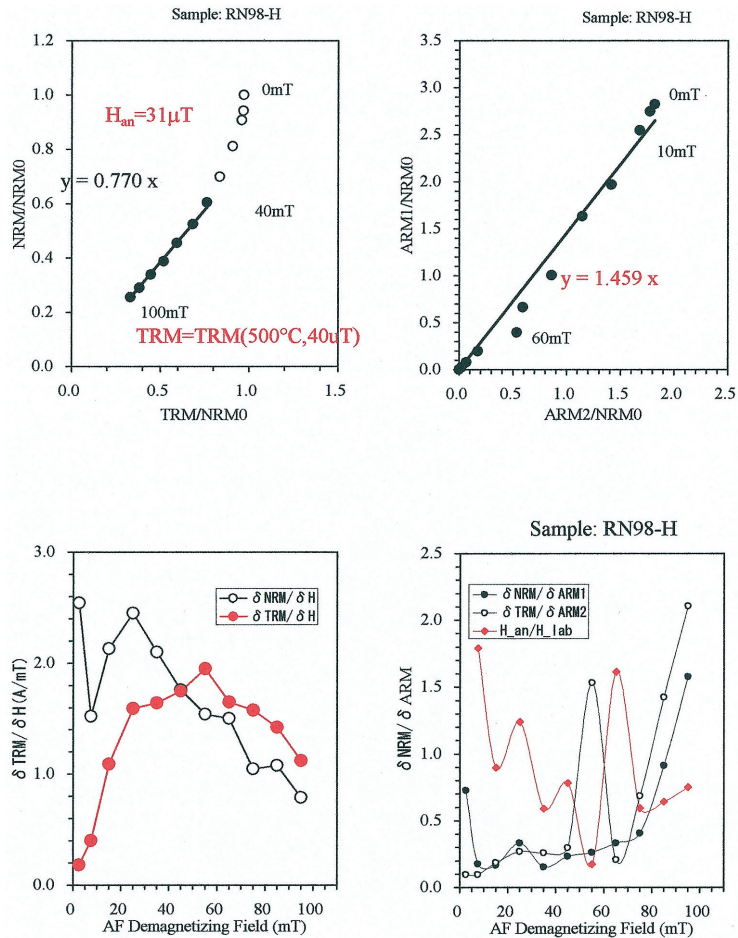


Fig. 11 Case study of Shaw's method on high density block of RN98_H

4. Results and discussion

From nine thermal stable specimens of Reunion 1998 lava, a good result of geomagnetic intensity of $36.1 \pm 1.9 \mu\text{T}$ was obtained by using Zheng's method and $37.7 \pm 4.2 \mu\text{T}$ by using differentiated Thelliers' method. For reference, the local field is calculated to $36.4 \mu\text{T}$ at Piton de la Fournaise ($h=2630\text{m}$, 21.14S , 55.43E) based on IGRF 2000 model (<http://wdc.kugi.kyoto-u.ac.jp/igrf/point/index.html>).

The good agreement of both methods of Zheng's and Thelliers' is due to no significant disturbing effect of magnetostatic interaction between grains appeared during the experiments.

Acknowledgements

Experiments were carried in the Natural Science Laboratory of Toyo university using VSM and Laboratory of Geological Analysis, Earth Science Division, Sogokaihatu Co.,Ltd using Sogo model fine-TD thermal demagnetizer and Agico JR-5A magnetometer, LDA-3A AF demagnetizer.

Sampling was carried out during the field excursion promoted by the IAVCEI 1998. The title of the excursion was A6: Volcanic Geology of Reunion Island, Indian Ocean. We appreciate to the organization members of the excursion, Drs. P. Bachelery, P. Mairine, T. Staudacher, V. Ferrazzini and K. Aki.

References

- Day, R., M.D. Fuller and V.A. Schmidt (1977), Hysteresis properties of titanomagnetites: grain size and composition dependence. *Phys Earth Planet Inter.*13:260-266.
- Pike, C., A.P. Roberts, K.L. Verosub and M.J. Dekkers (2001), An investigation of multidomain hysteresis mechanisms using FORC diagram. *Phys Earth Planet Inter.*126:13-28.
- Staudacher, T. (1998), Volcanic geology of Reunion Island, Indian Ocean: Field excursion guide book of IAVCEI'98 congress.
- Ueno, N., Z. Zheng, K. Nemoto and T. Hatta (2008), Thermal analysis of initial susceptibility, isothermal remanence magnetization, surface analysis by X-ray photoelectron spectroscopy and paleointensity determination by the new method, on Unzen Volcanic rocks. *J.Toyo Univ. Natural Science*, 52:117-148.
- Ueno, N. and Z. Zheng (2010). A case study of Unzen volcanic rocks by using Zheng's method for paleointensity determination. *J.Toyo Univ. Natural Science*, 54:107-145.
- Zheng, Z. and X. Zhao (2006), A new approach for absolute paleointensity determination: Consideration on blocking processes between temperature and interaction field. *EOS*

Trans.AGU, 87 (52), Fall Meet. Suppl., Abstract GP21A-1290.

Zheng, Z., X. Zhao and N. Ueno (2005), (in Japanese with English abstract) (鄭、趙、上野) テリエ法実験における強磁性粒子の非理想挙動の検出と補正。地学雑誌、114(2):258-272.

Zijderveld, J.D.A. (1967), A.C. demagnetization of rocks: Analysis of results. In Methods in Paleomagnetism, ed. D.W. Collinson, K.M. Creer & S.K. Runcorn, 254-286. Elsevier, Amsterdam.

要 旨

レ・ユニオン島 1998 年噴出溶岩の地球磁場強度と磁気特性

上野直子・鄭 重

鄭によって開発された古地球磁場強度測定法を用いて、1998年に噴出したレ・ユニオン島玄武岩について、その古地磁気強度を測定した。最も熱安定性の高い9試料から、 $36.1 \pm 1.9 \mu\text{T}$ の非常に良い値が得られた。また、この9試料から微分テリエ法で得られた古地球磁場強度は $37.7 \pm 4.2 \mu\text{T}$ であった。なお、標準地磁気モデル IGRF による2000年のレ・ユニオン島の地球磁場強度は $36.4 \mu\text{T}$ である。